LUDWIG MAXIMILIANS-UNIVERSITÄT MÜNCHEN
FAKULTÄT FÜR GEOWISSENSCHAFTEN

BACHELORARBEIT

Wissenschaftliche Arbeit zur Erlangung des akademischen Grades Bachelor of Science

eingereicht am Department für Geographie

Explorative Modeling of Aeolian sediment influx from surrounding sand pits into Lake Saint-Charles, Québec

Explorative Modellierung des äolischen Sedimenteintrags der umliegenden Sandgruben in den Saint-Charles See, Québec

Verfasserin:
Luzie Scheinpflug
Wangener Straße 55
82319 Starnberg
Luzie_Scheinpflug@gmx.de

Betreuer:
Prof. Dr. Ralf Ludwig
Mitbetreuung:
Richard Leduc, Ph.D.
Sonja Behmel

Datum: 22.8.2016

ABSTRACT

Lake Saint-Charles, situated north-west of Québec City in eastern Canada, is the largest drinking water reservoir for the city and supplies water to 300 000 residents. In recent years its trophic state has deteriorated and a premature aging has begun, placing the lake in an advanced mesotrophic state. Whilst the surface waters of Lake Saint-Charles have been closely monitored in the past, groundwater and atmospheric deposition have not been studied despite their great importance in understanding the state of the lake.

Explorative modeling alongside with a field work campaign were conducted to quantify total suspended particles (TSP) concentrations and potential deposition on the lake coming from a nearby sand and gravel pit. TSP emissions from the sandpit were calculated with the air dispersion model AERMOD. Necessary information to define sources and calculate their emission rates were mainly estimated. The field work campaign included three high volume samplers placed in a linear progression in a SW wind direction channel, ideally showing the increase of TSP after the sandpit compared to the control and the concentration that is potentially found over the lake.

Field work results showed no significant differences between the control station and the lake station, suggesting that no suspended particles from the sandpit reach the lake. No significant difference between sampling days with favorable and non-favorable wind conditions and wet and dry sampling days existed either. The very short sampling period and the small result count may be responsible for this result. The modeling showed an influx of TSP concentration and deposition onto the lake. The total estimated deposit of TSP on the lake was 1.16 t for the sampling period. Whether they originated from the sandpit or other activities in the surrounding area needs to be validated in further studies. It has to be noted that in the study area major road works and construction were under way. Local meteorological data and extensive knowledge concerning the sandpit's activity need to be made available to calculate more accurate results. Potential limnological impacts for Lake Saint-Charles can only be assumed at this point. It has to be noted that the TSP concentrations stayed under existing air quality standards. However, these standards do not take potential impacts on lakes into account.

This project has contributed to establish the necessary improved method for long-term monitoring of the impact of atmospheric depositions. Based on this explorative study, the City of Québec and the Association pour la protection de l'environnement du Lac Saint-Charles et les Marais du Nord (APEL) (responsible for the monitoring activities in the area) will be able to install the necessary equipment, collect the missing information on the sandpits' activities and to improve the monitoring methodology tested in this study.

I. Table of contents

II. List of tables

III. List of figures

1. Introduction

Monitoring of freshwater ecosystems and their water quality has become vital in recent decades, with evermore sources of anthropogenic pollution emerging and a growing world population increasing stress on natural resources. Pollutants can be transported through a system by air, water, soil and biota. The Aeolian pathway, representing the only transport not restricted to topographic boundaries, plays perhaps the most important role in the local, regional and global distribution of contaminants. It also allows relocation of particles within hours compared to the very time-consuming processes of soil infiltration and biological dispersal (Griffin et al. 2001; Park et al. 2004; Pope & Dockery 2006; Csavina et al. 2012). To monitor only surface water when it comes to understanding a lake may not be sufficient in order to take effective protective measures. New studies urge the need of a more holistic approach where groundwater and atmospheric deposition are included in lake monitoring programs (Fleckenstein et al. 2013; Schwoerbel & Brendelberger 2013).

Total suspended particles (TSP) reduce visibility and have a widespread impact on ecosystems. A subcategory of TSP comprises respirable particles with a diameter under 2.5 µm (PM25) (Avanti 2011; Csavina et al. 2011). These, being small enough to be breathed into lungs, represent a great health risk to humans, causing respiratory problems. Many human-induced activities, such as agriculture, use of motor vehicles and mining contribute large amounts to atmospheric dust concentrations (Csavina et al. 2012).

This study focuses on an exploratory modeling of TSP concentrations emerging from sand and gravel pits and the potential particle and nutrient input to Lake Saint-Charles and a field work campaign to quantify TSP concentrations on-site. The lake, which serves as a drinking water reservoir for Québec City, is well monitored for surface waters and land use and many possible sources of pollution have been documented. However, atmospheric depositions have not yet been monitored nor quantified. The main objectives of the study can be formulated as two key questions: 1) Is dust prevalent from the sand pit transported as far as the lake? 2) Can an increase of atmospheric particulate matter be directly measured north-east of the sand pit towards Lake Saint-Charles?

The environmental impact of TSP or Aeolian dust on freshwater has received very little research attention in recent years, while broader scientific studies are focused on human impact and respiratory health. In addition, nitrogen is dominantly transported in the atmosphere and thus much research has been carried out in terrestrial ecosystems known to be nitrogen-limited. Freshwater ecosystems, however, have not yet been broadly studied, as they are considered to be generally limited by phosphorus (Elser 2009). Still, some studies consider that atmospheric depositions may impact water transparency (Green et al. 2012) and can also contain phosphorus (Ellis et al. 2015). Recent studies have also shown that even though nitrogen is generally not the limiting factor, additional nitrogen input

from human activities can affect the natural balance of nitrogen and phosphorus ratios – with several potential impacts on the ecosystem (Schlesinger 1997; Glibert 2014).

Environmental modeling, especially air quality modeling, has gained importance with global awareness of pollution and climate change. To model air pollution levels, dispersion models were developed to calculate atmospheric pollutant concentrations prevalent from specific sources. This focus on dispersion first emerged during World War I and was further increased by World War II. Field work methods were dominant until computational development in the 1960s lead to atmospheric dispersion modeling (Jones 2004). The present day state-of-the-art approach of ensemble modeling is extremely relevant to dispersion modeling, as different types of models show different limitations and no model with the most accurate systematic performance can be highlighted (Galmarini 2007). Different types of models exist. Box models (e.g. Photochemical Box Model) represent a simple approach, modeling uniform inside "the box" or "an air packet" with minimal meteorological data. These are unsuitable for local environments influenced by small scale weather patterns as they do not provide point specific concentrations. Gaussian models (e.g. CALPUFF, AERMOD) are the most common regulatory models in North America. They calculate emission plumes based on steady state approximations, which represent hourly averaged meteorological situations assumed for all receptors within the modeling domain. This limits their productivity to small scale modeling extents. In addition they are traditionally unable to model the atmospheric chemical and physical processes that alters the pollutants. Recent developments, however, have allowed basic aspects of chemistry to be incorporated (e.g. CALPUFF). For instance, the Langrangian modeling approach (e.g. AUSTAL) enables to pursue the trajectory downwind whilst incorporating changes in concentration and chemistry of the initial air composition. The AUSTAL model is the regulatory air dispersion model of the official German Federal Environmental Agency (UBA 2016). Also, Computational Fluid Dynamic models (e.g. MISKAM, FLUENT) run under the assumption that pollutant dilution is equal in all directions and compute fluid flow by resolving the Navier-Stokes equation in three-dimensional finite circumstances. These models are thus suited for fine-scale scenarios (Holmes 2006).

However, as no model can yet compute values accurately on larger scales, it is indispensable to model small regions individually with local meteorological data. To our knowledge, no such study has been done at Lake Saint-Charles in the past.

A description of the study area from a physical-geographic point of view including its hydrology, geology and climate, an overview of land use and existing environmental problems is given in section 1.1. Subsequently an introduction to Aeolian sediments follows (section 1.2), before methods are explained in detail (section 2). The results and methods are then discussed, including potential limnological impacts on Lake Saint-Charles (section 3). Finally, the conclusion will point out possible applications of this study to future research and mitigation strategies (section 4).

1.1 Study area

The study area is situated 20 km north-west of Québec City, Canada. It encompasses Lake Saint-Charles and a sand and gravel pit located in its vicinity but which is situated outside of the lake's watershed. The water catchment of Saint-Charles river provides drinking water for 300 000 residents of Québec City, making it the most important drinking water resource of the region. Within this catchment, Lake Saint-Charles is the main reservoir and needs to be protected from further contamination and eutrophication (APEL 2014). Figure 1 shows a geographical overview of the study area and its location in eastern Canada.

Figure 1 Geographical overview of Lake Saint-Charles location in the province of Québec in eastern Canada.

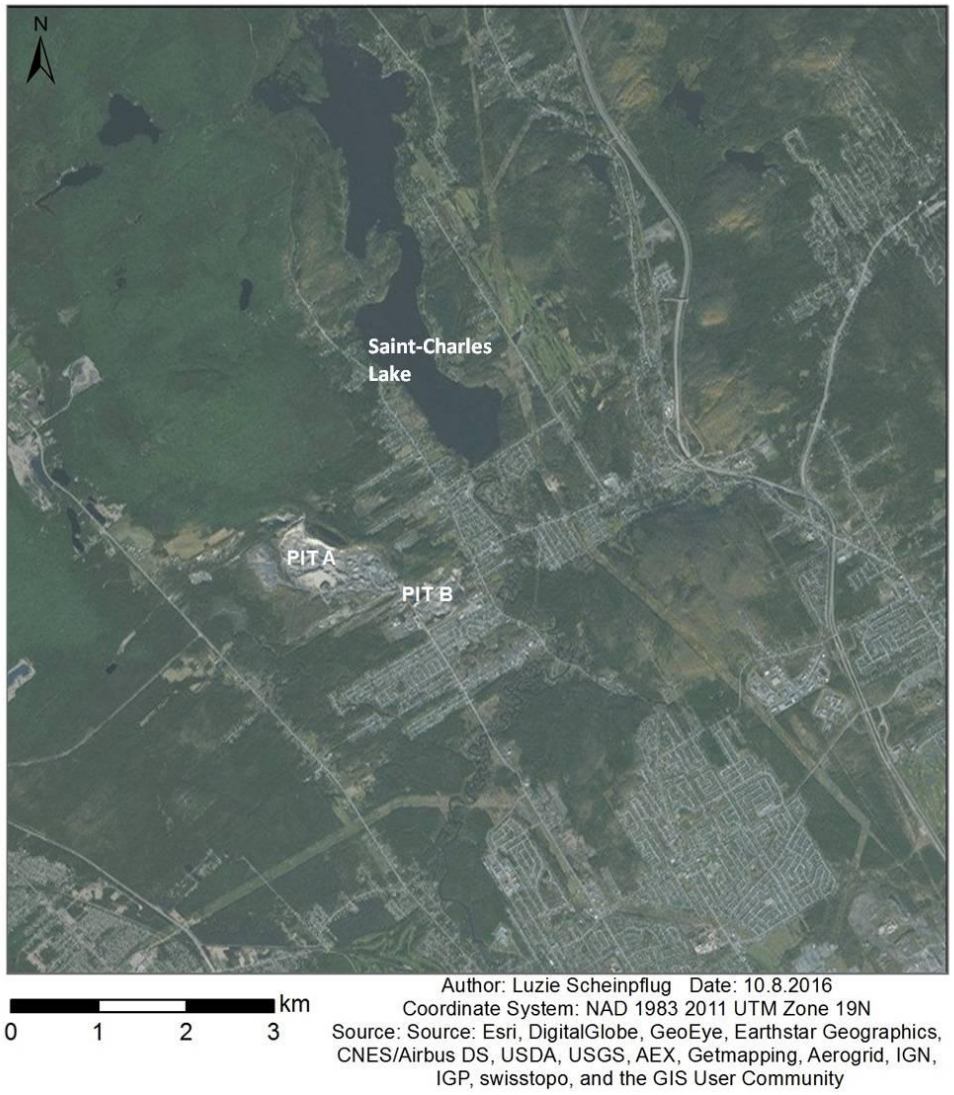

Figure 2 Map of the study area including the northern and southern basin of Lake Saint Charles and the studied sand pit to the south-west. Source: Carte interactive de la Ville de Québec.

Figure 2 shows Lake Saint-Charles including the sizable sandpit to the south-west. The observed sandpit is divided into multiple sub-pits, Pit A and Pit B (fig. 2). The larger open pit, Pit A (1400 m × 510 m) is operated exclusively for excavation of sand and gravel, whilst Pit B (600 m × 240 m), the smaller open pit, receives material assumingly for filling of older galleries. To the north-east, east and south-east the pit is embedded in a residential area. The dominating land cover to the north and west is forest. The surface area of the pit is estimated at 0.94 km^2. A simplified sandpit's workflow is derived from the US EPA AP 42 Section: 11.9.1. Sand and Gravel processing (1995). After excavation, the raw material is transported to a hopper, where large boulders are screened out. Conveyers transport the screened material to crushers for fine crushing. The material is then washed to remove organic impurities and clay. Afterwards the sand is dewatered and filled into dump trucks who distribute the material to clients.

1.2.1 Hydrology

Lake Saint-Charles has a surface area of 3.6 km^2 and is divided into two basins of different morphometry. The natural extend of the lake is limited to the northern basin where 70% of the total water volume, 14 810 000 m^3, is held (APEL 2009). The southern basin was created in 1934 after a dam was constructed to increase the volume of this reservoir, to respond to the increasing demand of the City. This construction raised water levels by 1.5 to 2 m, submerging the surrounding flatlands and initiating the onset of anthropogenic modifications to the lake's ecology and its water quality (Tremblay et al. 2001). The dam was raised a second time in the 1950's by an additional 2 m for equal reasons and with the same impacts on the lake's ecology.

This man-made southern basin is comparatively shallow at a maximum depth of 5 m, whilst the northern basin reaches depths up to 17.5 m. Figure 3 shows the bathymetry of Lake Saint-Charles today, demonstrating the distinct difference between the two basins. Water renewal rates are at 49.74 days in the northern basin and 21.01 days in the southern basin (APEL 2015). It should be noted that all presented data on water renewal rates represent average values. Further hydrological characteristics of both basins are given in Table 1.

In the northern basin sedimentation is of lacustrine nature with fine sediments settling in the still water. The south basin, being morphometrically different follows a fluvial sedimentation pattern. The main tributary is the Hurons River, which contributes 81.6% of the lake water. Other minor tributaries include the effluent of Lake Delage and 38 nameless streams (APEL 2014).

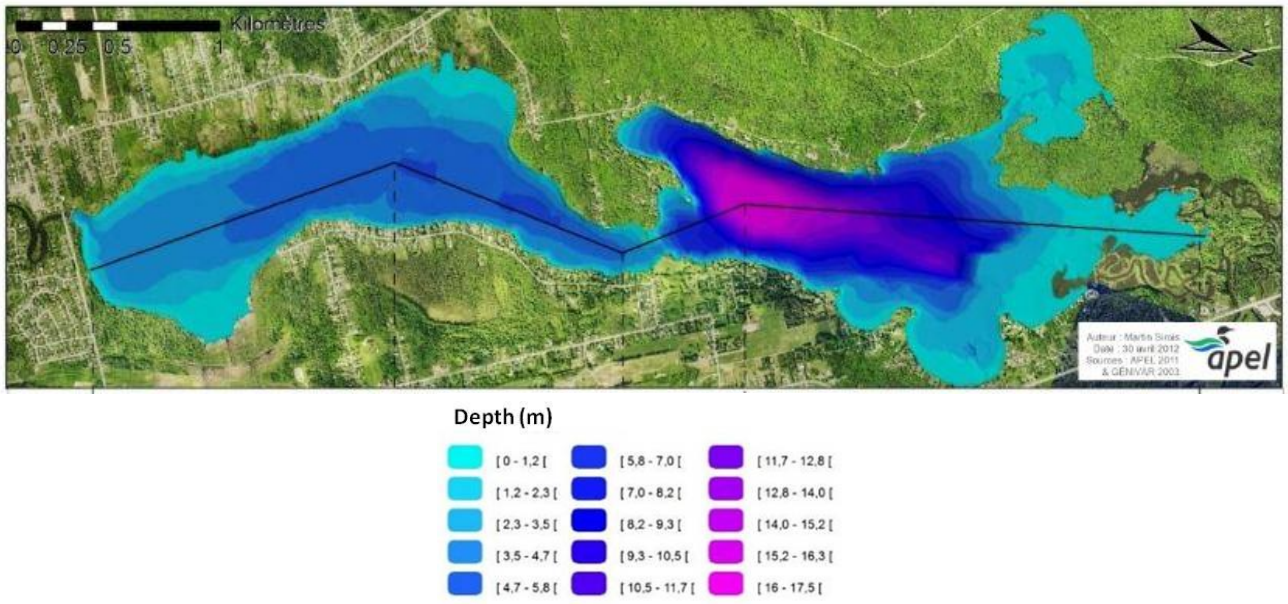

Figure 3: Bathymetry of Lake Saint-Charles.

Table 1: An overview of hydrological characteristics of Lake Saint-Charles two basins, the northern and the southern one. Source: APEL 2015.

	Lake Saint-Charles	Southern basin	Northern basin
Perimeter (m)	21347	8361	13244
Surface area (m^2)	3596587	1631886	1964702
Volume (m^3)	14836443	4579869	10237077
Maximum depth (m)	17.5	6	17.5
Average depth (m)	4.13	2.81	5.21
Maximum length (m)	5584	2911	2956
Maximum width (m)	1248	933	1290

1.2.2 Geology and Topography

The study area is situated entirely on the Precambrian shield. Lake Saint-Charles is embedded in a glacial depression shaped by the continental Laurentide Ice Sheet about 12 000 years ago during the Wisconsin glacial stage and later by the postglacial Champlain Sea. Sand and silt are the main deposits of glacial-lacustrine nature dating from that period (Bouchard 1988; Magnusson et al. 1997; Tremblay et al. 2001). However, the sandpit lies within an area of fluvio-glacial sediments of mainly sand and gravel (APEL 2009). The Wisconsin glacial stage is equivalent to the Würm glacial stage in European terminology.

The terrain east and west of the lake is slightly elevated with hills reaching heights between 150 to 450 m. However, the southern and south-western extremities of the lake are flat (Tremblay et al. 2001), creating a natural channel where wind speeds can increase (fig. 4). It is important to note that the observed sandpit lies south-west of the lake, in line with this wind-encouraging channel.

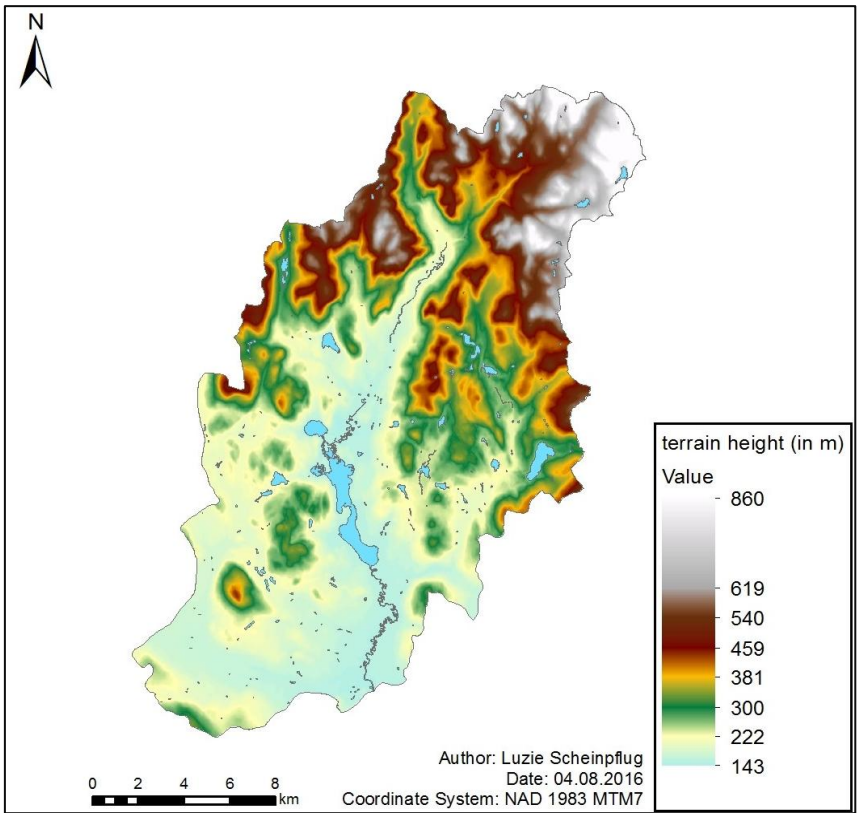

Figure 4: Topographic map showing terrain heights. Lake Saint-Charles lies in the middle of a wind encouraging channel from SW to NE. (Source: APEL)

1.2.3 Climate

Situated in the St-Lawrence river valley, Lake Saint-Charles and its surroundings lie within the mixed wood plains ecozone, the smallest of Canada's 15 terrestrial ecozones (ESWG 1995). Its climate is characterized by the Köppen taxonomy as humid continental within the temperate midlatitudes (APEL 2014; Schultz 2005). Temperatures are considered temperate, compared to the northern Boreal zone and the southern subtropical ecozones. Diurnal temperature ranges are pronounced with the warmest month July reaching an average temperature of 19.3°C and winter temperatures with an average of -12.5°C in January (Environnement Canada 2015; Schultz 2005).

Average annual precipitation is relatively high at 1189.7 mm with no clear seasonal or annual variations. During the winter season, from October to April, most of the precipitation will fall as snow (Environnement Canada 2015; Schultz 2005). January and February are the snowiest months with 74% and 80% of the precipitation falling as snow, whilst about 24% of the annual precipitation is in the form of snow (Government of Canada 2016). During the snow cover time the sandpit is not operating and thus no emissions are produced. The growing season is restricted to an average of 165 days per year (Bourget 2011). Typical vegetation in the region includes mixed forests of sugar maple, red maple, eastern hemlock, black ash, white spruce, yellow birch, tamarack, eastern white cedar and eastern white pine (ESWG 1995).

The influence of wind is of great importance to this study. When plotting the wind rose for average wind speed and direction data of the weather station located at Jean-Lesage International Airport Québec 22 km to the south, dominant wind directions become clear (fig. 10, p. 25). Wind flow in the directions SW and NE, in line with the wind encouraging channel described in section 1.2.2 (fig. 4), will have an impact on lake Saint-Charles by transporting TSP into the water catchment area. In the absence of local meteorological data, the wind directions observed from the airport data are assumed to prevail, thus implying that remote sources outside the catchment can contribute to the hydrological closed system. As a reminder, the observed sandpit lies outside the defined water catchment boundary but within the wind flow zone.

1.2.4 Land Use

Land use in the watershed of Lake Saint-Charles is considered anthropogenically shaped although 77% are still forested areas. The lake catchment extends over three municipalities: Cantons-unis de Stoneham-et-Tewkesbury, Québec city and the city of Lac-Delage. The population has been steadily increasing with a sharp rise in the 1970s. An estimate in 2013 approximated the population at 10 000 (APEL 2014). Figure 5 gives a cartographic overview of land use of the Lake Saint-Charles catchment, whilst Table 2 shows the specific percentage coverage of individual land uses. The lake sides consist of shallow slopes which allows residential and commercial development built close to the shoreline (Tremblay et al. 2001). It is estimated that 4084 housing units are built within 500 m of the water bodies, of which 1784 have septic tanks installed and are not linked to the local sewage line (APEL 2014). The region has also experienced touristic development. A ski resort and a golf course cover 1.87% of the total area. In addition a few natural parks, like Marais du Nord and Parc linéaire de la Rivière-Saint-Charles, host predominantly day tourists year-round. Natural environments, including forests, water and wetlands are still dominant in the catchment area. However, even though anthropogenic land use represents only a small percentage of the total area, it has a significant environmental impact on water quality and ecology in the region. The lake's environmental problems are discussed in chapter 2.5.

Table 2: Land use classes of the watershed of Lake Saint-Charles and their respective surface area in square kilometers and percent. Source: APEL 2014.

Land use class	Surface area (in km^2)	Surface area (in %)
Vegetation (forest)	130.29	76.62
Open areas	13.12	7.72
Water	6.53	3.84
Wetlands	5.52	3.25
Slash/burning areas	3.72	2.19
Carriage way	3.71	2.18
Barren land	1.51	0.89
Agriculture	1.47	0.86
Sandpits	1.31	0.77
Golf courses	1.01	0.59
Ski runs	0.86	0.51
Buildings	0.70	0.41
Landfills	0.19	0.11
Infrastructure	0.05	0.02
Junkyards	0.03	0.02
Swimming pools	0.03	0.02
Total	***170.05***	***100***

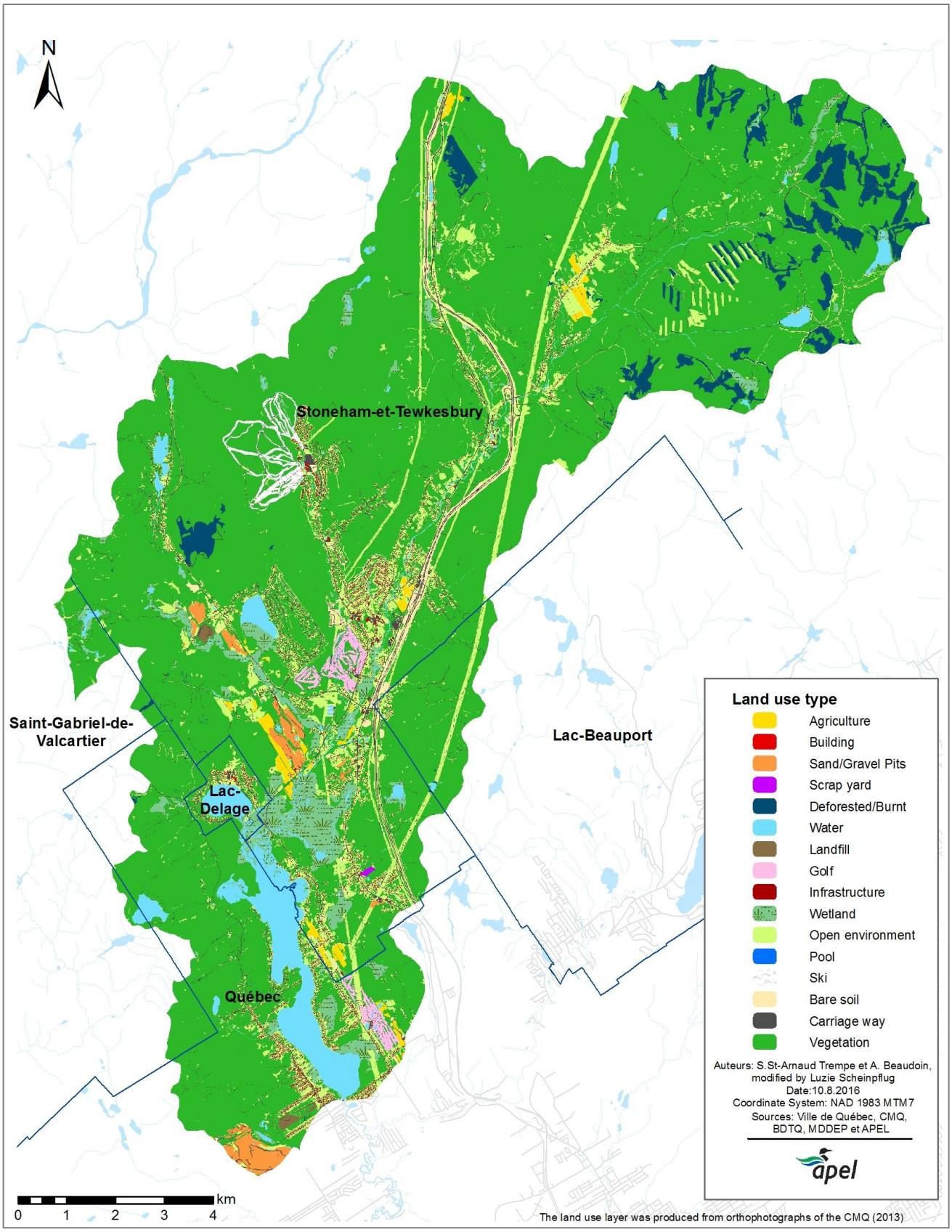

Figure 5: Land use map of the watershed of Lake Saint-Charles. Sources: Ville de Québec, CMQ, BDTG, MDDEP et APEL.

1.2.5 Environmental problems

Lake Saint-Charles is currently under a lot of strain, both as a drinking water resource and a natural ecosystem. In recent years the lake's trophic status has been rapidly degrading. Recent residential developments and the construction of a highway have contributed to its degradation through erosion during construction and additional road salt applications since (APEL 2014). In addition, waste water treatment is not optimal within the watershed considering that 1784 residences are on septic installations. It was mentioned in chapter 1.2.4 that a significant amount of housing units are not linked to the local sewage line and have septic tanks instead. Water treatment of these outdated septic tanks is generally not biological and most houses are built too close to the lake or its main tributaries. The remaining are connected to two municipal waste-water treatment plants (aerated lagoons only) that discharge their effluents upstream of lake Saint-Charles. In fact, one of the plants actually discharges directly into the lake whilst the other discharges a few hundred meters upstream (APEL 2014).

Due to a gradual but continuous increase in nutrient supply, the lake's trophic state has deteriorated, initiating the onset of a premature aging. Its current trophic condition is classified as advanced mesotrophic. Eutrophication is a natural phenomenon defined as the augmentation of primary plant production following an abundant nutrient supply.

Lakes in particular are prone to eutrophication considering the long residence times of the water compared to rivers and streams, where a lot of water movement takes place. Lake Saint-Charles, however, has a very short residence time, which is a possible reason for not deteriorating faster (Rolland et al. 2013). Following an increased nutrient supply, aquatic plant production generally increases and with that the demand for oxygen and the organic sedimentation rate. The latter will further fuel the process of self-eutrophication acting as another source of phosphorus (Schwoerbel & Brendelberger 2013).

Concerning Lake Saint-Charles, an acute proliferation of aquatic plants was observed between 2007 and 2012, covering 44.6% of the lake's surface and indicating the onset of eutrophication. Another indicator of human-induced eutrophication is the presence of cyanobacteria. A first surface appearance of cyanobacteria colonies on the lake was observed in August 2006. Since then, they have occurred every year with significant temporal and spatial variance (APEL 2014). Cyanobacteria are potentially toxic as some species produce cyanotoxines (Chorus et al. 2000; Cox et al. 2005; Ernst et al. 2005) which can cause damage to for example the nervous system and the liver (Carmichael 2001). Water treatment costs rise significantly when a drinking water reservoir is prone to cyanobacteria blooms (Jüttner & Watson 2007; Steffenson 2008). Indeed, following the blooms of 2006, the water treatment plant of Québec was upgraded with significant financial investments reference (APEL 2014).

Furthermore, land use modifications have permanently changed discharge patterns in the water catchment. The construction of road axes has reduced infiltration thus augmenting discharge flow rates. Higher, localized discharge concentrations increase soil erosion, carrying large sediment amounts towards the water. The proximity of roads increases water concentrations of oils, road salts, petroleum, heavy metals and dust, especially from construction and unpaved roads (APEL 2014). According to Yannopoulos (2013) lead, zinc and cooper are the most important heavy metal pollutants in freshwater ecosystems. Chlorides are found in de-icing road salts, which also include sulfur, sodium and calcium (Yannopoulos et al. 2013). Therefore, during the winter months, chlorides also represent an abundant pollutant in road discharges. Heavy metal and chloride concentrations are currently researched by APEL and cannot yet be confirmed.

Touristic establishments in the area like a golf course and ski slopes reduce infiltration and increase erosion, influx of nutritive elements, pesticides, herbicides and discharge speed.

Sand quarry exploitation near a water body may cause additional dust and nutrient depositions through Aeolian and hydrous sediment influx and may thus increase turbidity and nutrient inflow (APEL 2014; Peckenham et al 2008).

1.2 General introduction to Aeolian sediments

Natural environments prone to Aeolian processes mainly include deserts and coastal zones. Wind erosion, including abrasion and deflation (Csavina et al. 2012), and transport of Aeolian sediments depend on vegetation cover, wind and fine particle supply. Strong winds and sparse or no vegetation cover favor ablation of an area. In contrast to such natural erosion zones, anthropogenic landforms affected by wind erosion are agricultural fields in times of no or sparse planting (Lancaster 2009), pastures, open pit mines including sand or gravel pits, dirt roads and construction activities. An educated assumption that anthropogenically altered surfaces are especially sensitive to wind erosion can be made, however, their contribution to the global atmospheric dust load is widely disputed and varies between factors of under 10% up to 50% (Csavina et al. 2012; Goudie & Middleton 2006). TSP originating from natural dust sources often contain insignificant amounts of contaminants (Zobeck and Fryrear 1986; van Pelt and Zobeck 2007; Reheis et al. 2009).

By definition atmospheric particulate matter is heterogeneous in structure, source and chemical nature and can only be categorized by particle size (Grantz et al. 2003). Sand and gravel mining, in the form of open pit mining or light charge blasting, emits large quantities of Aeolian dust and TSP. Material handling, crushing and transport as well as large, heavy vehicles along haul roads induce dust emissions. Although meteorological factors such as prolonged dry weather and strong winds increase emissions, it is important to note that mining of such pits generates a continuous dust discharge (AVANTI Mining Inc. 2011; Csavina et al. 2012). Dust transported from such sand and gravel pits,

mining sites and dirt roads is often referred to as fugitive dust, as it leaves the boundaries of its original point source (Goudie & Middleton 2006). As previously mentioned in the introduction, the Aeolian pathway is the most rapid and boundless transport mechanism for particles and aerosols. Especially particles with low volatility or low aqueous solubility rely on wind displacement (Csavina et al. 2012).

Three different types of Aeolian sediment transport have been identified based mainly on particle diameter (fig. 6): 1. surface creep, 2. saltation and 3. suspension (Lancaster 2009; Field et al. 2010). Larger particles (diameter > 500 µm) are displaced by a rolling motion called surface creep or reptation. Particles ranging from 20-500 µm diameters are transported via saltation, a short term suspension as a series of hops. Saltation displacement can reach distances of hundreds of meters. Small particles (diameter < 20 µm) can reach a state of total suspension in the air depending on settling velocity and atmospheric turbulence (Goudie & Middleton 2006; Lancaster 2009; AVANTI Mining Inc. 2011).They can either be uplifted into the atmosphere directly or as a consequence of saltation and surface creep. Large particles colliding with the soil create enough kinetic energy for cohesive forces to falter, rendering more particles accessible for wind-driven deflation (Shao et al. 1993).

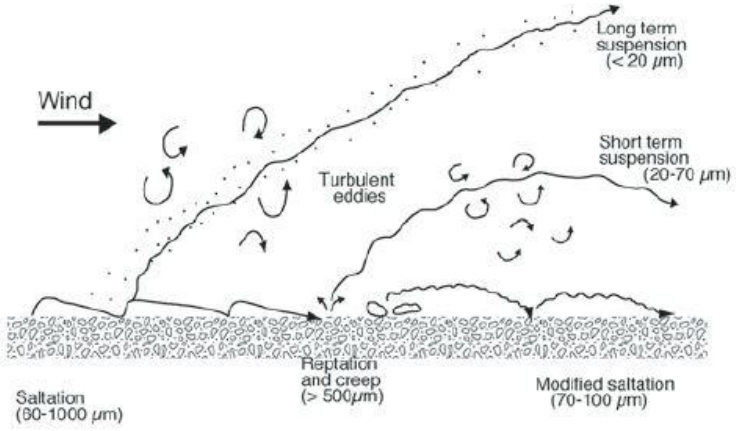

Figure 6: Types of Aeolian transport dependent on particle diameter. Source: Lancaster 2009.

TSP can be transported on local, regional and even global scales, for example Sahelian dust reaching Europe and even the Americas (Stuut et al. 2009). Larger particles are often deposited in close proximity of the source, whilst finer particulate matter remains volatile for longer time periods and distances (SENES Consultants LTD 2013). From an environmental point of view, Aeolian sediments have not yet been studied as extensively as other pollution sources. The chemical composition of Aeolian sediments varies notably between sources depending on soil composition, bed rock and land use. However, a strong correlation between particle size and certain chemical characteristics exits. For example most organic matter like sulfur or nitrogen derivatives are attached to finer particles, whilst coarser particles carry heavy metals and base cations (Grantz et al. 2012).

This study focused on suspended particulate matter from the observed sand pit carried towards the lake. TSP air concentration and deposition, which include all particles less than 44 μm (SENES 2013) were measured and their distribution modeled.

2. Materials and Methods

2.1 Materials

Three high volume samplers (Hi-Vol) were provided from the Québec Ministry of Sustainable Development, Environment and Climate Change (Ministère du Développement durable, Environnement et Lutte contre les changements climatiques - MDDELCC). The ministry also contributed NEWTERRA 4 inch recording charts for a time period of 24 hours. Laboratory costs were covered by the City of Québec. The laboratory used was EXOVA Canada, which provided pre-weighed cellulose air filters with plastic bags for storage. Wood pallets and weights to secure the Hi-Vol safely were provided from APEL and volunteers. APEL also provided a SUUNTO clinometer. AirMet Science Inc. sponsored a trial version of the Lakes Environmental model AERMOD 9.1.0.

2.2 Field work

Alongside the modeling of an emission plume, TSP concentrations were measured with Hi-Vols. Three Hi-Vols were installed in a linear progression, ideally showing the increase of TSP after the sandpit compared to the control and the concentration that is potentially found over the lake (fig. 7). As explained in chapter 2.2, a natural wind encouraging channel from south-west to north-east exists in the test area. The Hi-Vols were installed in line with this passage. Samples were recorded every three days over a period of 24 hours (midnight to midnight). Every other sampling period coincided with those of the National Air Pollution Surveillance Program Canada (NAPS) who record every six days. The field work campaign ran from May 15th 2016 to August 1st 2016.

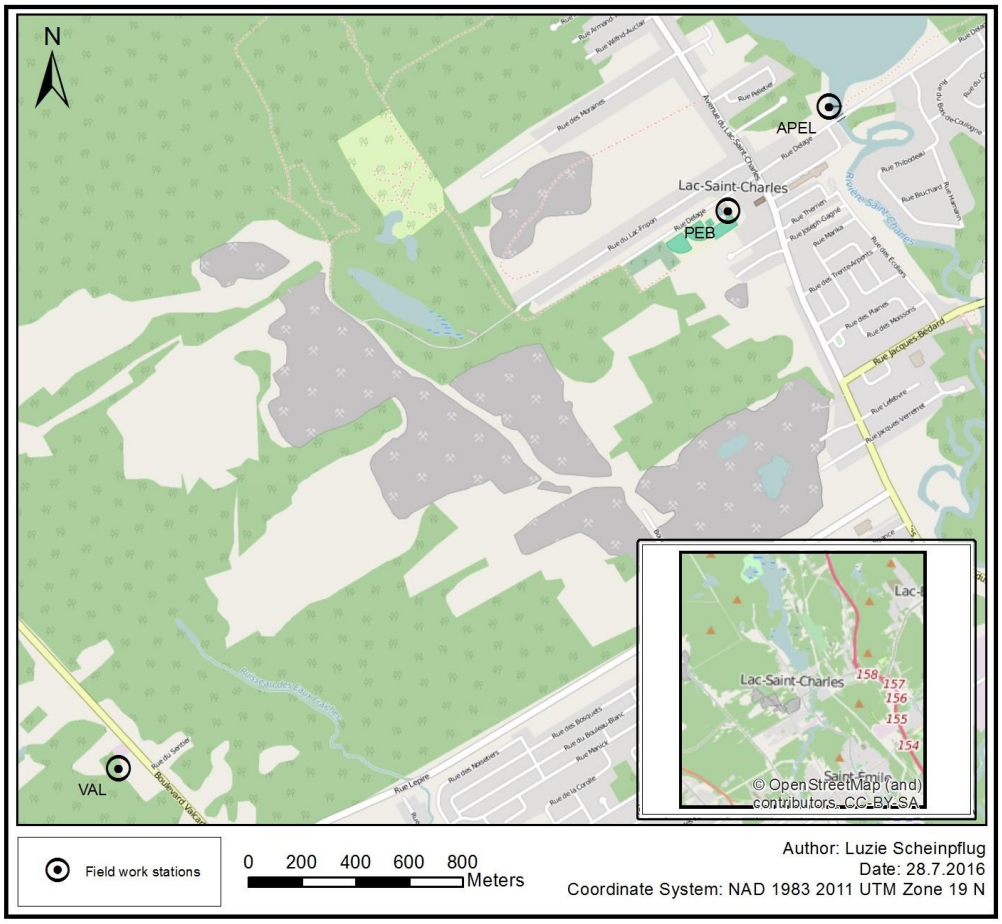

Figure 7: Overview map of the three field work stations placed in a linear progression. VAL represents the control site. PEB and APEL are strategically placed north-east of the sand pit to measure particle transport by wind towards lake Saint-Charles.

Figure 8: Showing surroundings of the three Hi-Vols. Figure 8a) shows the surroundings of the third Hi-Vol at the site APEL, installed on the control center of the embankment dam at Lake Saint-Charles. Figure 8b) shows the location of Hi-Vol PEB. It is situated on a two story community center. A construction site can be seen in the Hi-Vols immediate surroundings. Figure 8c) shows the landscape surrounding the control site VAL. It is situated in a private backyard on a lawned area. The white arrows represent north arrows for orientation purposes within the panoramas.

Test sites were chosen for their strategic placement but also by their accessibility and practicality. The first Hi-Vol, *VAL*, the site representing the control, is situated in a private backyard on a lawned area at UTM 19N 316729 5195540. The surrounding area consists of a man-made landscape of lawn, shrubbery and trees (fig. 8a). This Hi-Vol was installed to the south west of the main boulevard Valcartier to reduce road dust pollution of the control by dominantly south-west winds.

The second Hi-Vol was installed on top of the Paul-Émile-Beaulieu Community center, UTM 19N 319006 5197604. Located in close proximity, north-east of the sand pit, dust concentrations were expected to be highest at this test site dubbed *PEB*. Here the Hi-Vol was mounted on the roof of the high two-story building (fig. 8b). The site PEB is situated in a residential area with recreational sports fields and a pool attached to the community center.

The third test site, *APEL*, was placed on the control center of the embankment dam at the outflow of lake Saint-Charles into the Saint-Charles river at UTM 19N 319384 5197991. The surroundings include APEL's office building, a small recreational area, residential houses and the lake (fig. 8c).

The Hi-Vols were equipped with a vacuum pump, a recorder for the air volume passed through the filter and a timer (fig. 9). The vacuum pump sucked air through the filter over a period of 24 hours where dust particles are accumulated. To attain a concentration value ($\mu g/Rm^3$) after the filter's analysis the air volume needed to be recorded and monitored (fig. 9b). The timer allowed the filters to be changed at any time between periods and ensure a timely onset of the sampling period.

Different types of filters exist: cellulose, glass fiber and teflon. Here cellulose filters were used. When changing a filter (fig. 9c), caution needed to be taken to not break cellulose filters and thus altering the weight ratio. Tweezers were used to remove fragments of the filters from the grid which remained in place after it was removed. The filters were folded and stored in airtight plastic bags, in their respective envelopes in which they came in from the lab. Start, end and average air volume values were stated on the envelope for the lab's analysis. The total concentration of TSP was deduced of pre- and post-weight of filters after sampling days. The post weight was determined after a minimum of 24 hours dessication.

A local temporary meteorology tower installed by the Institute national de la recherche scientifique (INRS) gave information on the daily dominant wind direction and precipitation. Sampling days with dominant wind directions S, SSW, SW and SSE were later taken into account for statistical analysis.

Field work results were statistically analyzed with Sigma Plot and Microsoft Excel. Note that besides the TSP concentration, nitrate (NO_3) and sulfate (SO_4) concentrations were also analyzed in the laboratory. The dried filters were completely immersed in distilled water to dissolve NO_3 and SO_4 ions. The solution was then analyzed with ionic chromatography to separate the ions and deduce their weight and concentration. However, due to the limited time of the project and the long duration of

analysis, these values were not included in this study. However, a quick statistical analysis can be found in Appendix B.

Figure 9: Figure 9a) shows the Hi-Vol at *VAL* on its wooden pallet stand with brick weight enforcements. Figure 9b) shows the timer (top) and the air volume recorder (bottom) that manually draws the measured volume on an exchangeable 24 hours recording chart. Figure 9c) shows the top of a cellulose filter placed on the vacuum pump.

2.2.1 Meteorology

A temporary meteorology tower was installed on the roof of the control center of the embankment dam, close to the *APEL* Hi-Vol. Daily dominant wind directions and precipitation data were used for the field work campaign to determine relevant sampling days (winds prevalent from the south). Table 3 shows the dominant wind directions and their respective frequencies over the course of the field work campaign. Winds coming from the south are the most prevalent, followed by north-east winds.

Table 3: Wind direction frequencies on sampling days measured at the temporary meteorological tower at *APEL*.

Wind direction	Number of sampling days	Frequency (%)
NE	7	25.00%
SSE	4	14.29%
S	10	35.71%
NW	5	17.86%
N	1	3.57%
W	1	3.57%
Total	**28**	**100.00%**

2.3 Modeling

The regulatory short range air dispersion model, U.S. EPA AERMOD, was used to determine ambient air concentrations of TSP in proximity of the discussed sand pit. AERMOD is "a steady-state plume model that incorporates air dispersion based on planetary boundary layer turbulence structure and scaling concepts, including treatment of both surface and elevated sources, and both simple and complex terrain" (EPA 2016). It is applicable to multiple emission sources including volume, area, point and line sources, and both in urban and rural settings. A steady-state plume model calculates concentrations at certain receptors for one single temporally averaged meteorological value of the hour regardless of their position within the modeling extend. AERMOD is dependent on two pre-processors, AERMET and AERMAP. AERMET's inputs (wind speed, wind direction, temperature, cloud cover, albedo, surface roughness and Bowen ratio) are needed to calculate planetary boundary layer (PBL) parameters, which are later used by the AERMOD internal meteorological interface to generate meteorological profiles. AERMAP generates terrain and receptor data of each individual receptor defined by the user using a Digital Elevation Model (DEM). It calculates the receptor's representative terrain-influence height (h_c), location and height above mean sea level and passes the information on to AERMOD. Figure 10 describes the modeling system in a simple diagram (EPA 2004).

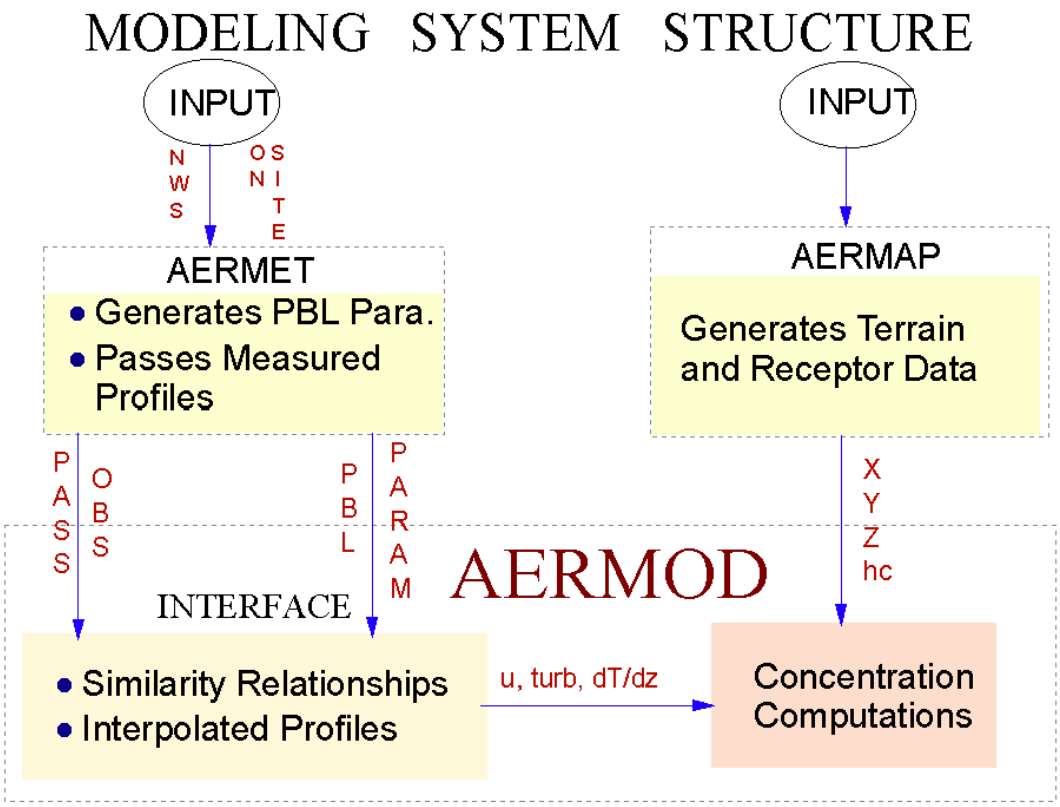

Figure 10: A workflow diagram of the AERMOD modeling system structure showing the two pre-processors AERMET and AERMAP. AERMET output (Planetary Boundary layers and passes measured profiles) are fed into the AERMOD file, where modeling extent, pollutants, receptors, sources and time frames are defined. Before computation, AERMAP's terrain data is applied to previous defined receptors. AERMOD computes its output concentrations. (Source EPA 2004)

Since AERMOD follows the same computational patterns when modelling in flat and complex terrain, it is not necessary to specify the terrain type. Two possible limiting states of the boundary layer are modeled; a horizontal, terrain impacting plume and a terrain-following plume. The two layers are divided by the streamline height (H_c) (EPA 2004). These two states are weighed relatively to the given meteorological conditions to form one sum of concentrations (Venkatram et al. 2001). Stable conditions favor the horizontal plume, otherwise in neutral or unstable conditions the terrain-following plume dominates. The conditions depend on the wind speed, the degree of atmospheric stability and the plume height relative to the terrain. A general concentration equation is given below:

$$C_T\{x_r, y_r, z_r\} = f \times C_{c,s}\{x_r, y_r, z_r\} + (1 - f)C_{c,s}\{x_r, y_r, z_p\}$$

C_T $\{x_r, y_r, z_r\}$ represents the total concentration. The contribution from the horizontal plume and the terrain-following plume are $C_{c,s}$ $\{x_r, y_r, z_r\}$ and $C_{c,s}$ $\{x_r, y_r, z_p\}$ respectively. The subscripts c and s are associated to convective and stable atmospheric conditions. $\{x_r, y_r, z_r\}$ defines the receptor coordinate. Note that z_r is defined relative to the stack base elevation (particle release height), whereas z_t is the actual terrain height at the receptor calculated via AERMAP. The height coordinate z_p in the terrain-following plume is attained by $z_p = z_r - z_t$. Evidently in flat terrain $z_t = 0$ and $z_p = z_r$, so deductively the concentration is defined only by the horizontal plume. When calculating z_p only the lowest height where a streamline can be maintained due to sufficient kinetic energy is needed. f is the plume state weighting function, deciding which state is dominant (EPA 2004).

2.3.1 Emission rate calculation

AERMOD requires emission rates to be calculated manually beforehand to later appoint them to their respective sources. These were calculated for TSP and PM25. The pit's annual operation period is estimated from the 15th of April to the 30th of November excluding weekends and based on the onset of local snow cover, resulting in a total of 163 working days per year. The excavated soil's humidity was estimated at 3% and its silt content at 10% based on a finger probe and literature values. Emission rate calculations were handled corresponding to the US EPA AP-42 guidelines of the U.S Environmental Protection Agency and thus divided into the following groups: mobile sources, material handling and heavy machinery, and wind erosion. The sand pit was divided into sub-pits PIT A and PIT B (fig. 11). Whilst emission factors are simple to calculate for point sources like chimneys, emission factors of more complex sources are given by the US EPA for the purpose of calculating emission rates.

Mobile sources

Two days of counting and classifying trucks entering and leaving the sand pit built the data basis for this calculation. As the sand pit has multiple entries both survey points were chosen carefully in order to maximize passing trucks. Passing trucks were categorized by tire count, use and their direction.

Three main vehicle groups were established and a truck model representative of each group was later chosen to specify weight and size dimensions (tab. 5). Maximum weight capacity was set at the province of Québec's road weight limits. 10-wheel dump trucks were placed in the weight category A3, whilst 14-wheel and 22-wheel semitrailer dump trucks were placed in the weight categories A12 and A68 respectively. The truck route through the pits, as seen in figure 9, was devised to cover all heavy machinery and apparent active surfaces as seen on satellite images. Where two ways were possible, the total amount of trucks was simply divided in half. The total length of segments added up to 3969.1 m. Table 4 shows the length of all individual segments, whilst figure 11 shows a map of the segments throughout the sandpit.

Table 4: Length of unpaved road segments that trucks cover in sandpit. The segments are obtained by separating the truck route into significant parts at turning points and intersections.

Segment	Length (m)	Segment	Length (m)
AB	106.5	*BI*	164.9
BC	459.5	*IJ*	139.9
CD	168.4	*IK*	90.8
DE	286.5	*JL*	95.2
EF	259.7	*KL*	155.2
EG	364.6	*LM*	284.8
GH	377.1	*MM*	323.2
HD	240.5	*MB*	474.1

It was observed that 10-wheel and 14-wheel dump trucks only passed through PIT A, whilst 22-wheel semi-trailer dump trucks were exclusively present in PIT B. A grader was assumed to pass once a day to level all unpaved roads in the pit. Its speed (S) was set at 10 km/h. The grader's emission rate was calculated in agreement with the US EPA AP-42 Section 11.9: Western Surface Coal Mining.

$$E_{TSP} = 0.0034 \times S^{2.5}$$

$$E_{PM2.5} = 0.031 \times E_{TSP}$$

S = speed of grader = 10 km/h

In addition, water trucks passed on the road segments AB and BC irrigating them and thus reducing their emission factors by 95% (US EPA AP 42 1995). Pick-ups, mechanic and petrol trucks were counted and assumed to pass on all road segments. Table 5 shows the weight specifications and dimensions as well as the number of daily journeys for each vehicle class.

Table 5: Vehicle Class specifications, including make and model, dimensions, weight and the number of daily journey's within the sand pit. Source: gritindustries.com, uship.com, oldaussivolvos.com (15.6.2016), legisquebec.gouv.qc.ca (16.6.2016).

Vehicle class	Model	Dimensions (m)	Empty weight (t)	Loaded weight (t)	Average weight (t)	Number of daily journeys
10-wheel dump truck	VOLVO WCA64T	8.23*2.49*3.28	23.58	32	27.79	67
14-wheel dump truck	VOLVO N12	11.46*2.43*2.75	26.31	41.5	33.91	151
22-wheel semi-trailer dump truck	TRIAXEL End dump + chassis	17.07*2.59*4.04	22.5	57.5	40	120
Water/ irrigation trucks	Peterbilt 365	6*2.6*3.2	29.94	49.94	39.94	2
Pick-ups	Ford F-250	5.9*2.7*2.0	3.5	n/a	3.5	1
Mechanic	Peterbilt 348	8.3*2.6*2.7	27.22	27.3	27.26	1
Petrol truck	Peterbilt 365	6*2.6*3.2	29.94	49.94	39.94	10
Grader	Caterpillar 160M	n.a.	n.a.	n.a.	19.76	1

Emission factors for road segments were calculated according to the US EPA AP-42 Section 13.2.2: Unpaved Roads. Emitted particles from unpaved surfaces at industrial sites are defined by the following equation:

$$E = k\left(\frac{s}{12}\right)^{a} \times \left(\frac{W}{2.72}\right)^{b}$$

This equation was adapted to European units. The variables k, a and b represent empirical constants listed in Table 6.

E = size-specific emission factor (kg/VKT), VKT = vehicle kilometer travelled

s = surface material silt content (%)

W = mean vehicle weight (metric tons)

Table 6: Constants specified by the US EPA to calculate vehicle dust emission factors. Source: US EPA AP-42, 1995.

CONSTANT	PM2.5	TSP
k (kg/VKT)	0.042	1.381
a	0.9	0.7
b	0.45	0.45

E_s first needed to be multiplied by the annual total VKT to create an emission factor per year before being converted into g/s. The final step was to add the separately calculated grader emission factor (g/s). Individual emission factors were calculated for each road segment.

Material handling and heavy machinery

Total material handled in the pit per day was determined from the trucks' capacities and their number of daily journeys, assuming that workloads are always equal throughout the year, and trucks are always loaded to their maximum legal capacity. Material handling includes charging and discharging of trucks and is calculated according to the equation given in the US EPA AP-42 Section 13.2.4: Aggregate Handling and Storage Piles.

$$E = k(0.0016)\frac{\left(\frac{U}{2.2}\right)^{1.3}}{\left(\frac{M}{2}\right)^{1.4}}$$

In this equation, the following variables are defined as:

E = emission factor (kg/t)

k = particle size multiplier (dimensionless)

U = mean wind speed (m/s)

M = material moisture content (%)

The variable k is dependent on the aerodynamic particle size range (tab. 7).

Table 7: Aerodynamic Particle Size Multiplier for TSP and PM 2.5. Source: US EPA AP-42, 1995.

Aerodynamic particle size	Aerodynamic Particle Size Multiplier (k)
TSP (< 30 µm)	0.74
PM2.5 (< 2.5 µm)	0.053

Hourly wind speed data from 1st of January 2008 to 31st of December 2012 measured at the weather station of Québec International Airport Jean-Lesage were used to generate monthly mean wind speeds. Emission factors for heavy equipment processes were given in the US EPA AP42 Section 11.19.2: Crushed Stone Processing and Pulverized Mineral Processing (tab. 8).

Table 8: Emission factors of heavy equipment processes. Source: US EPA AP-42, 1995.

Emission factor	conveyer transfer point	fine crushing
TSP (< 30 µm)	0.0015	0.0195
PM2.5 (< 2.5 µm)	0.00055	0.0075

It was assumed that only fine crushing was necessary due to the original small particle size of the sand and gravel particles extracted. The emission factors for material handling and heavy machinery were added together resulting in a total factor for each open pit source.

Wind erosion

Active surfaces of open pit mines, such as discharge cones, bulldozed areas and excavation pits, are affected by wind erosion. However, wind speeds need to exceed 19.3 km/h (WSP 2014) in order to ensure a larger wind shear velocity at the soil surface than the soil aggregates' shear strength (Gillette et al. 1980; Shao 2008). The surface area of all active surfaces apparent on satellite pictures was measured and added together to form a pseudo surface equivalent to the annual active surfaces. The annual active surfaces of OPITA and OPITB are 31 157.09 m^2 and 14 142.94 m^2 respectively. These were divided by 12 to create monthly values. Emission factors were calculated according to the following equations, where S represents the silt content:

$$E_{TSP} = 1.51 \times 10^{-5} \times S$$

$$E_{PM25} = 0.2 \times E_{TSP}$$

Here the unit of the emission factor E is $g/s/m^2$.

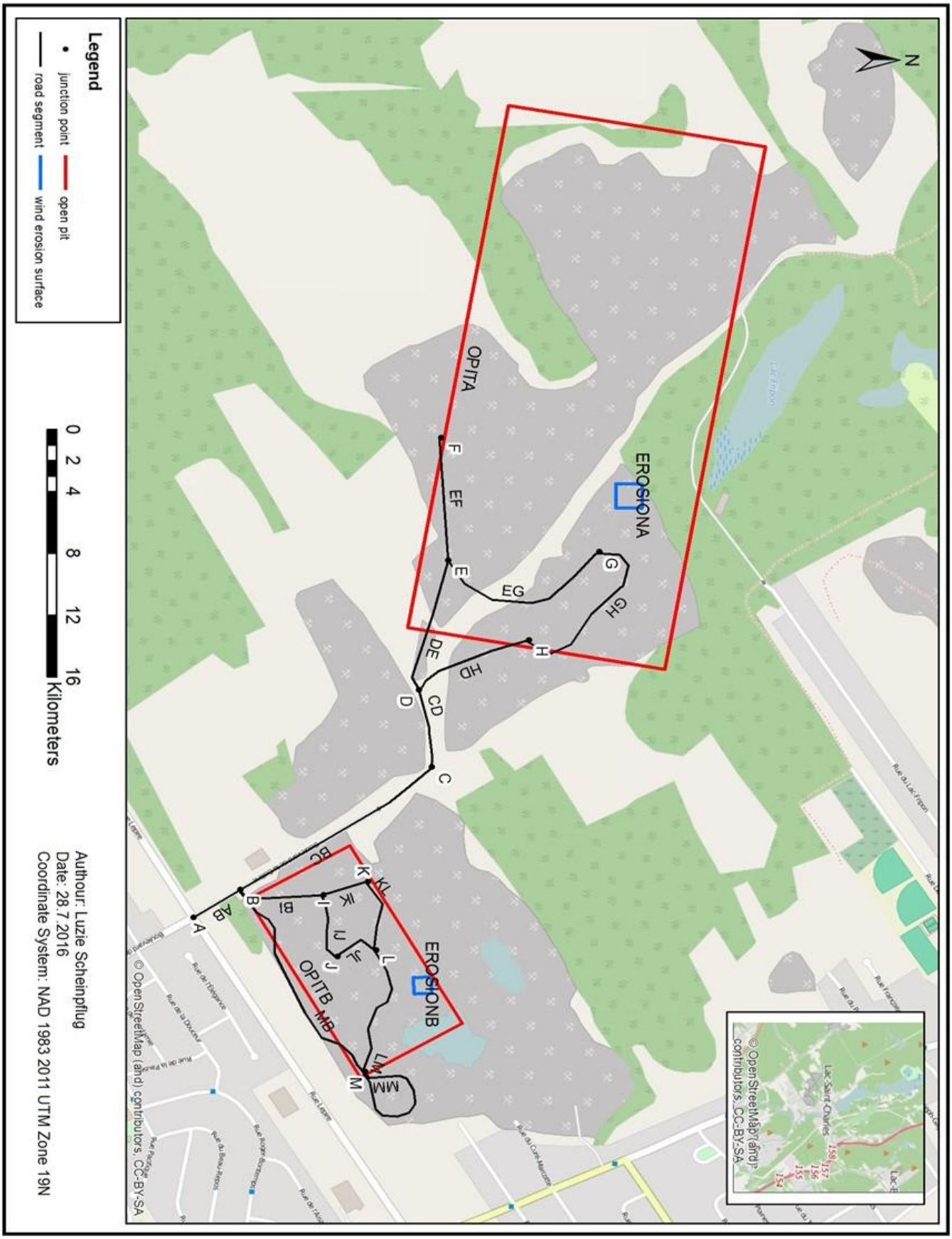

Figure 11: General site map of sandpit with all sources, including wind erosion surface area sources, open pit sources and line volume sources, specified. Open pit A is the larger, northern pit. Open pit B is the smaller pit to the south.

2.3.2 Meteorology

As mentioned earlier, AERMOD requires hourly meteorological standard data (EPA, 2004). The data used was taken over a five-year time period from 1st of January 2008 to 31st of December 2012 collected at the weather station of Québec International Airport Jean-Lesage (Station number 16294). Upper air data was retrieved from Maniwaki, Québec (Station number 4734). All data was collected from the MDDELCC. Figure 12 and table 9 show wind direction frequencies over the 5-year period. The dominant wind directions are visualized in figure 12 as south-west and north-east. However, local meteorology data would be of great importance.

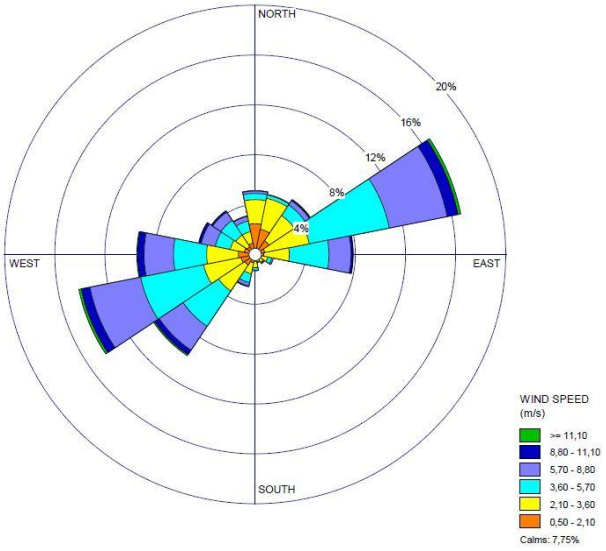

Figure 12: Wind rose visualising the dominant wind directions, NE and SW. Data source: MDDELCC, 1.1.2008 - 31.12.2012, Jean-Lesage International Airport Québec.

Table 9: Wind directions and their respective frequencies over the 5-year period from 1.1.2008 to 31.12.2012 at Jean-Lesage International Airport Québec. Of specific interest are the wind directions SSE, S, SSW, SW and WSW (29.67%). Data source: MDDELCC.

Wind direction	%	Wind direction	%
N	4.89	*S*	1.14
NNE	4.79	*SSW*	2.23
NE	5.13	*SW*	10.08
ENE	16.58	*WSW*	15.64
E	6.86	*W*	10.09
ESE	1.26	*WNW*	4.76
SE	0.77	*NW*	4.33
SSE	0.58	*NNW*	3.22

		CALM	7.63

For this study, wind directions SSE, S, SSW, SW and WSW are of importance because they carry the Aeolian deposits from the sand pit towards the lake. Altogether 29.67% of the time, wind promotes particle displacement from the sand pit towards the lake. Table 10 shows the wind speed characteristics over the 5-year period.

Table 10: Average monthly wind speeds in km/h, m/s and their maximums measured to determine when wind erosion is possible (wind speeds > 19.3 km/h). Data source: climate.weather.gc.ca, 1.1.2008 - 31.12.2012, Jean-Lesage International Airport Québec.

Month	**Wind speed**		
	km/h	*m/s*	*Max (m/s)*
Jan	16.91	4.70	5.44
Feb	16.64	4.62	5.14
Mar	15.42	4.28	5.14
Apr	16.05	4.46	4.44
May	14.26	3.96	4.44
Jun	12.79	3.55	4.00
Jul	11.94	3.32	3.44
Aug	12.01	3.34	4.44
Sep	11.69	3.25	3.44
Oct	14.96	4.15	4.86
Nov	13.32	3.70	4.72
Dec	15.35	4.26	5.28

2.3.3 Modeling parameters

Air concentration and dry deposition were modeled for a 5 by 5 km modeling extend centered over the office building of APEL (UTM 19N 319340 5197934). If not specified otherwise default settings were always used. The depletion type used was dry depletion. TSP was chosen as pollutant with averaging time options of 1-hour, 24-hour and a period, which is specified above as 163 days. The "RURAL" dispersion coefficient was chosen to reflect the study area's landscape. A total of 20 sources were defined, which were described more closely in chapter 2.3.1. They consist of 16 road segments, thus line volume sources, two open pit sources and two area sources to quantify wind erosion. The sources were grouped into roads, open pit and wind erosion to quantify the pollution contribution of specific parts of the pit's activity. Previously calculated emission rates were entered. The receptors, points for which the model calculated specific values, were specified as a nested grid with the characteristics represented in table 11. The bounding box is placed in the middle of the modeling domain.

Table 11: Receptor spacing of nested grid as specified for modeling in AERMOD.

Distance from Bounding Box (m)	Receptor Spacing (m)
200	50
500	50
1000	100
2000	200
5000	500

In addition three discrete Cartesian points were added at the field work stations, *VAL*, *PEB* and *APEL*. The meteorological files, surface met data (.sfc) and profile met data (.pfl), cover the characteristics described above in chapter 2.3.2 Meteorology. At this point the period of 163 days was specified in AERMOD. Wind speed categories were user specified. AERMOD default values were kept with the exception of category C. Here the original value was adapted to 5.36 m/s, which corresponds to the wind speed needed for significant wind erosion.

Table 12: User specified wind speed categories used by AERMOD. The wind speed values represent the upper limit of each category. Wind erosion is possible in categories D and E (hence factor 1.0).

Category	Maximum wind speed (m/s)	Factor
A	1.54	0.0
B	3.09	0.0
C	5.36	0.0
D	8.23	1.0
E	10.8	1.0

Different emission scenarios were set up. Both wind erosion area sources were defined to only emit in wind speed categories D and E (tab. 12) when the 19.3 km/h (5.36 m/s) threshold is reached. Furthermore, emissions of all other sources were limited to operation hours of 7 am to 7 pm on weekdays. Subsequently AERMOD's terrain processor, AERMAP, was run based on the WebGIS option *CDED 15-Min 1:50K (Canada - 23 m)*. This is a digital elevation model (DEM) produced from the Canadian Digital Elevation Data (CDED) by Natural Resources Canada, which is publically accessible free of cost. After base elevations for all sources were imported, they were modified manually to simulate the pit hole, which didn't show in the DEM. With a the use of a clinometer, the depth of Pit A and Pit B were estimated at about 82 and 18 m respectively. The base elevations of the road segment CD were changed to descend into the pit. The base elevations of all other road segments in Pit A were reduced to the lowest base elevation of segment CD of 85.15 m. The open pit and area source were also

set at 85.15 m. Regarding Pit B, the DEM showed values close to the original estimate of 18 m. Base elevations were thus not modified.

The model's deposition results were finally used to calculate an estimate of the dust quantity that falls into the lake per period. The lake was divided into trapezoids and squares, of which average depositions were calculated and later added up to a total deposition.

3. Results and Discussion

3.1 Field work

3.1.1 Field work results

Relevant field work results are displayed in table 13. All other results with wind directions other than S, SW, SSW and SSE can be found in Appendix A. Taken at face value, the results presented in table 13 may show an increasing progression from the VAL site to the PEB site and then a slight decrease at APEL. This result was anticipated, expecting dust emissions to increase after the sand pit at PEB and then decreasing at APEL due to partial deposition of these particles. However, a statistical analysis was needed to test these assumptions. The differences in dust quantity between days can be explained by weather conditions. After longer warm dry spells, a lot of dust is accumulated in the air, whilst on days with significant precipitation dust is flushed to the ground. On the 24th of May, construction was on-going at both PEB and APEL sites, probably contributing to the dust emission. All concentrations are probably underestimated due to micro-scale residue of the filters that remains stuck to the Hi-Vols.

Table 13: Collected field work results of sampling days with desired dominant wind directions: total concentration of TSP per 24 hour period and precipitation data of that day. Data source: APEL.

Date	Concentration (µg/Rm^3)			Dominant wind direction	Precipitation (mm)
	VAL	PEB	APEL		
18-05-2016	7.7	18.8	8.9	SSE	0.0
21-05-2016	22.6	38.6	31.8	SSE	0.0
24-05-2016	41.2	56.4	50	SSE	0.0
27-05-2016	23.2	32.8	27.9	S	6.9
30-05-2016	23	32.2	29.7	S	19
08-06-2016	10.8	14.5	17.7	S	0.3
11-06-2016	10.6	19.3	11	S	0.0
14-06-2016	16.7	22.7	21.1	SSE	0.3

23-06-2016	13	24.8	124.7	S	0.0
17-07-2016	14.9	23.1	45.7	S	0.3
23-07-2016	13.6	15.6	11.3	S	0.0
26-07-2016	12.6	17.1	15.5	S	0.3
29-07-2016	11.9	17.4	7	S	0.0
01-08-2016	15.1	40.8	12	S	0.0

Statistical characteristics, obtained through an analysis of variance (ANOVA) test, of the result groups VAL, PEB and APEL are shown in table 14. The Shapiro-Wilk Normality Test failed indicationg a non-gaussian distribution. Therefore median and percentiles are shown rather than means and standard deviations. Though it is observable in the percentiles that the values cover a large range, it is not clear from the Shapiro-Wilk Normality test whether a significant difference between the stations exist.

Table 14: Median and 25%/75% percentiles of relevant data collected at the three stations.

Value group	Median	25%	75%
VAL	14.250	11.625	22.700
PEB	22.900	17.325	34.250
APEL	19.400	11.225	35.275

The next step of the ANOVA test was a chi-squared test to test significant difference of the groups. An alpha level of significance of $P \leq 0.001$ and 2 degrees of freedom were determined. The calculated value for chi squared was $\chi^2 = 17.286$. As can be taken from table 15, the difference between the median values of the group are greater than would be expected by chance (red value), thus contradicting the null-hypothesis and proving a significant difference exists.

Table 15: Chi Square distribution table. Source: math.hws.edu/javamath/ryan/ChiSquare.html (2.8.2016).

Degree of freedom	0.5	0.1	0.05	0.02	0.01	0.001
1	0.455	2.706	3.841	5.412	6.635	10.827
2	1.386	4.605	5.991	7.824	9.210	13.815
3	2.366	6.251	7.815	9.837	11.345	16.268
4	3.357	7.779	9.488	11.668	13.277	18.465
5	4.351	9.236	11.07	13.388	15.086	20.517

Therefore the *Tukey Test*, a post-hoc all pair-wise multiple comparison procedure, was conducted to test the significant difference between stations. Whilst ANOVA can only determine if there is a significant difference, the *Tukey Test* is able to specify between which groups it exists (Hale & Astolfi 2015). Table 16 shows the test results. They are further visualized in figure 13.

Table 16: Tukey test results to test significant difference between result groups.

Comparison	Diff of Ranks	q	p	P < 0.050
PEB vs. VAL	22.000	5.880	<0.001	Yes
PEB vs. APEL	11.000	2.940	0.094	No
APEL vs. VAL	11.000	2.940	0.094	No

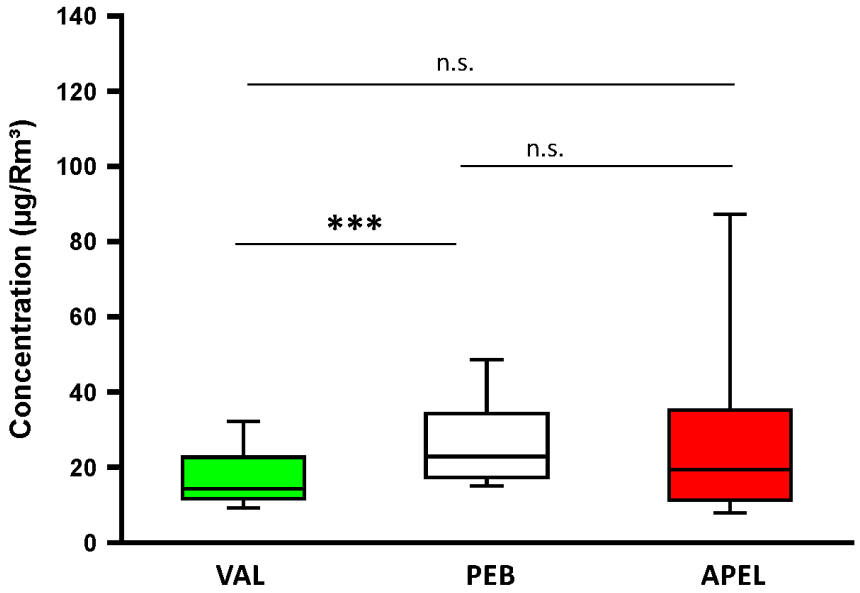

Figure 13: Box plot diagram to visualize the Tukey test results. * strong significant difference, n.s. no significant difference.**

The station pairs PEB and APEL, and VAL and APEL do not show a significant difference. However, the test VAL vs. PEB resulted in a significant difference, setting apart the control station from the first post-sand pit measurement. Since VAL and APEL do not show a significant difference, dust emissions from the sand pit towards the lake do not significantly exceed base concentrations before the sand pit and are thus negligible. Evidently over a longer period of time, a progression between PEB & APEL and VAL & APEL might become significant.

In addition to significance tests between the groups, the values of each station were classed into two groups, values on days with favorable dominant wind directions and values on days without, whose averages are shown in table 17. Favorable wind directions encourage dust transport from the sand pit

towards the Hi-Vol. The averages of the two groups were compared per station via a paired t-test to test their significant difference.

Table 17 Average value of data groups favorable and non-favorable concerning wind directions prevalent from the sandpit per field work station

Station	Average TSP concentration (µg/Rm^3)		Favorable wind directions
	favorable	non-favorable	
VAL	16.86	17.85	N, NE, ENE
PEB	26.87	36.06	W,WSW, SW, SSW, S, SSE
APEL	29.59	24.34	WSW, SW, SSW, S, SSE

The results of the t-test are shown in Table 18. In all three t-test of the individual groups the null hypothesis was retained, showing that the differences between the favorable and non-favorable data are not significantly different but completely due to chance. Thus dust influx on days with favorable wind conditions is statistically not different from on non-favorable days. This result contradicts the expectations that dust influx would be more prevalent from the sand pit and suggests that there is no significant dust augmentation on days with favorable wind conditions.

Table 18: t-test results of the data groups favorable and non-favorable concerning wind directions prevalent from the sand pit per field work station.

	VAL	PEB	APEL
t	-0.25	-0.97	0.59
Two-tailed Critical value	2.06	2.06	2.10
Significant difference	no	no	no

A further statistical analysis was conducted to test the influence of precipitation on TSP concentrations. The sampling days were classed into two groups, dry days (<1mm) and wet days (>1 mm). Again a paired t-test was used to test their significant difference for each station individually. Table 19 shows that once more no significant difference between the value groups exist and any variation is due to chance.

Table 19: t-test results of comparison between wet (> 1 mm) and dry (< 1 mm) sampling days.

	VAL	PEB	APEL
t	0.12	0.19	-0.11
Two-tailed Critical value	2.06	2.06	2.06
Significant difference	no	no	no

Much more data points need to be collected to perform a more plausible statistical analysis. For this study only 27 samples were taken at each station, however merely 14 of these sampling days had the necessary wind direction characteristics. Statistical outliers such as the concentration of 124.7 µg/Rm^3 at the APEL site on the 23rd of June (tab. 13) would be evened out by a sizable data collection. The fact that the t-tests for favorable/non-favorable wind directions and for wet/dry days did not show significant differences, strongly suggest that the sample size is too small. A larger field work campaign will probably show variations and gradients developing.

3.2.2 Method discussion

The fieldwork method mirrored the proceedings of the Canadian government department for Environment and Climate Change who conduct similar atmospheric dust concentration measurements across the country. The benefits and disadvantages of cellulose filters are versatile. They are very cost-effective, but also more fragile, ripping easily and sticking to the Hi-Vol's grids. This could alter the final weight thus rendering the results more imprecise. Large volumes of dust clog this type of filter causing pumps to overheat and malfunction due to a fast onset of large pressure drops, a problem less common with glass fiber filters. On days with large dust quantities, stable airflow rates may not be sustained throughout the sampling periods and may drop up to a factor of two.

Cellulose filters are organic, making it possible to analyze accumulated inorganic matter directly without prior separation from the filter (Dams & Heindryckx 1973). Under certain conditions, particularly on humid sampling days, fragments of the cellulose filters were lodged in the grids of the Hi-Vols impossible to remove even with tweezers. These samples are usually no longer usable. However, in order to attain a quantity of filters suitable for statistical analysis over the short field work period, they were nonetheless considered.

With the technology dating from the eighties, only manual timers are installed. Separate intervals measure 30 minutes, making it difficult to precisely adjust the beginning to midnight. An uncertainty of 15 minutes must be expected.

It is of importance to note that the control test site is still situated in an anthropogenically altered and exploited area and thus does not represent a completely natural baseline. Regrettably, an active construction site is situated next to the PEB filter, possibly contaminating filters with dust not prevalent

from the sand pit. At the lakeside site APEL landscaping works of the recreational area and road construction caused dust turbulences impacting the sampling days. All construction work was continuous of the course of the field work campaign from mid-May until the end of July. However, extraordinary peaks were not measured on construction days. For example on the 27th of May, landscaping works were taking part in close proximity to the APEL Hi-Vol, however, the measured concentration of 27.9 µg/Rm^3 is not significantly higher than on other sampling days. On the 2nd of June, the air volume recorder failed to measure the air volume at the station PEB, rendering that sample unusable.

The meteorological data is not standardized, since it was installed on a building and the structure can cause turbulences and thus influence the measured data. In the future a standardized meteorological tower will be installed to provide data for both the field work campaign and the modeling.

Generally, the field work campaign needs to be extended to attain enough data for a plausible statistical analysis. This study was confined to a very small time frame not covering a full work season of the sand pit. The data collected in this study provide pilot data for a large-scale investigation.

3.2 Modeling

3.2.1 Emission rate results

Emission rate results were calculated following the US EPA AP 42 guidelines as described in section 2.3.1 - Emission factor calculation. TSP values are naturally more elevated than PM25 values, as they incorporate a larger quantity of particles. PM25 particles are included in the TSP values. Tables 20 and 21 show the results of emission factor calculations.

Table 20 Emission rates of open pit sources calculated (including material handling and heavy equipment) according to the US EPA AP-42 guidelines.

	Particle size	Material handling (g/s)	Conveyer (g/s)	Crusher (g/s)	Total (g/s)
OPITA	*TSP*	0.704	1.200	15.605	17.510
	PM25	0.050	0.440	6.002	6.493
OPITB	*TSP*	1.035	1.167	n/a	2.201
	PM25	0.074	0.428	n/a	0.502

Table 21: Emission rates of line volume sources (road segments) calculated according to the US EPA AP-42 guidelines.

SEGMENT	TSP (g/s)	PM25 (g/s)	SEGMENT	TSP (g/s)	PM25 (g/s)
AB	6.653	0.195	*BI*	1.898	0.056
BC	18.015	0.528	*IJ*	0.826	0.024
CD	6.602	0.194	*IK*	0.515	0.015
DE	5.616	0.165	*JL*	0.562	0.016
EF	10.182	0.299	*KL*	0.880	0.026
EG	7.147	0.210	*LM*	3.293	0.097
GH	7.392	0.217	*MM*	3.663	0.107
HD	4.714	0.138	*MB*	5.482	0.161
			TOTAL	83.441	2.447

3.2.2 Model results

Results of the modeling of TSP air concentration and dry deposition are presented in figures 14 and 15. TSP air concentration from all sources is shown in figure 14a. Over the course of the 163 day period described in chapter 2.3.3, 1 µg/m^3 is modeled at the southern tip of lake Saint-Charles. Figures 14b and 14d show the open pit source contribution and the road source contribution respectively. Both figures have isolines of 0.5 µg/m^3 at the approximate location of the 1 µg/m^3 total concentration isoline, suggesting that both contribute equally to the total. Wind erosion (fig. 14.c) is much smaller influence with only 0.01 µg/m^3 reaching the most southern tip of the water body. Concentrations are really high closest to the pit. The dominant wind directions become especially clear in figure 14.c where the oval shape of the isolines corresponds to the SE and NW directions mainly found in this corridor. The dry deposition follows the same pattern as the concentration. Again open pit source and road source contribute approximately equally to the overall dry deposition which can be seen when comparing the isoline of 1 g/m^2 in figure 15a (total deposition), and the isolines of 0.5 g/m^2 in figures 15b (open pit deposition) and 15d (road deposition) respectively. Wind erosion becomes insignificant with a 0.005 g/m^2 deposition at the southern tip (fig. 15c). According to the resulting isolines, dust influx is of main importance to the southern basin of lake Saint-Charles. This basin is already only 4.5 m deep (APEL 2014) and is at risk of silting up with the dam installed at the discharge. Note that these figures show a periodical average over the estimated annual working days (163) of the sand pit. The 24 hour maximum results for both concentration and deposition were also modeled and are shown in figure 16.

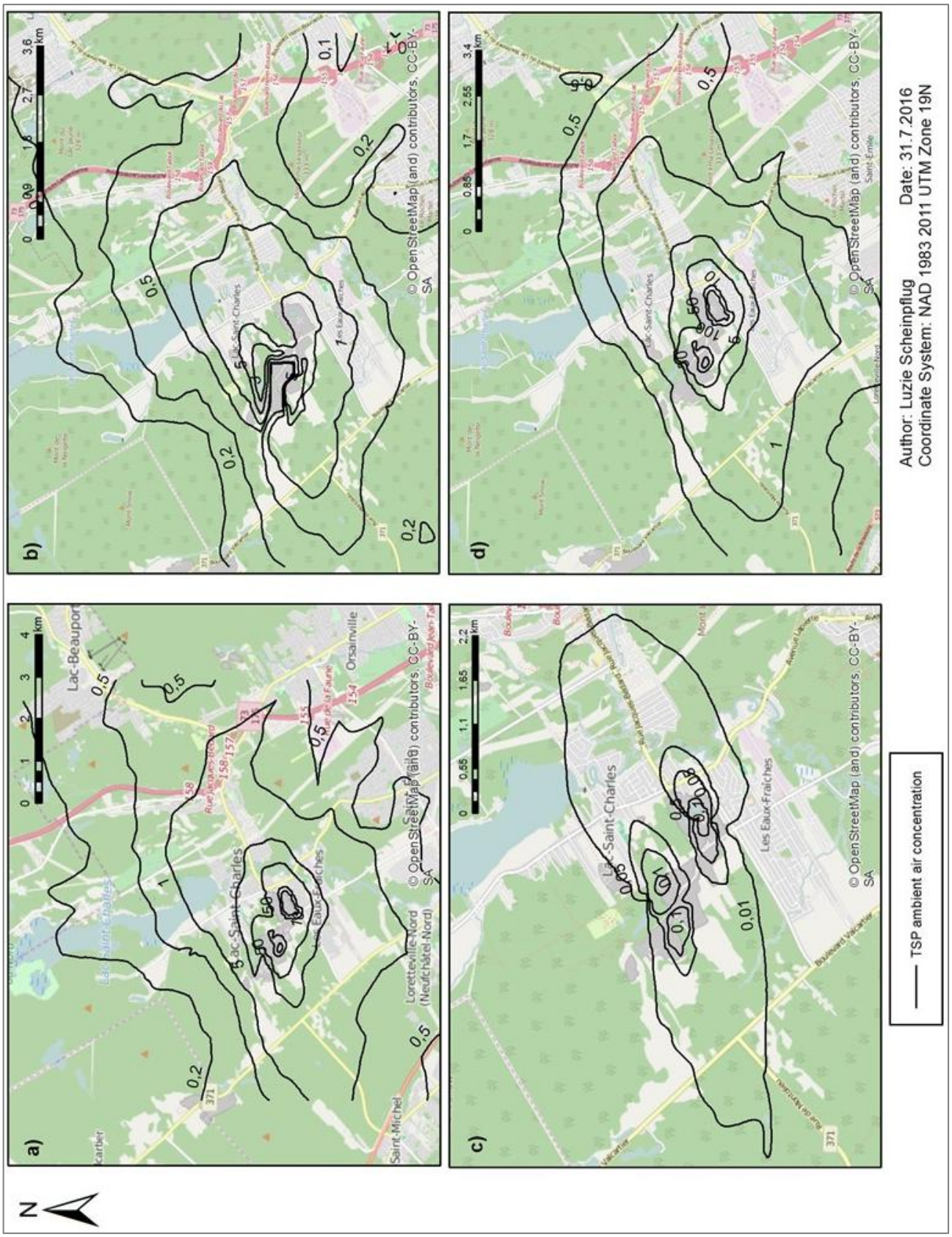

Figure 14: AERMOD modeling results of the TSP air concentration (µm/m^3). Figure 14a) represents the impact of all sources of the sand pit combined. Figure 14b) shows the significant contribution (about half) of the two open pit sources to the total concentration. Figure 14c) shows the impact of wind erosion on the air pollution, which is negligible. The emissions of the line sources (truck passage on road segments) are shown in figure 14d), representing also roughly half of the total emissions reaching Lake Saint-Charles.

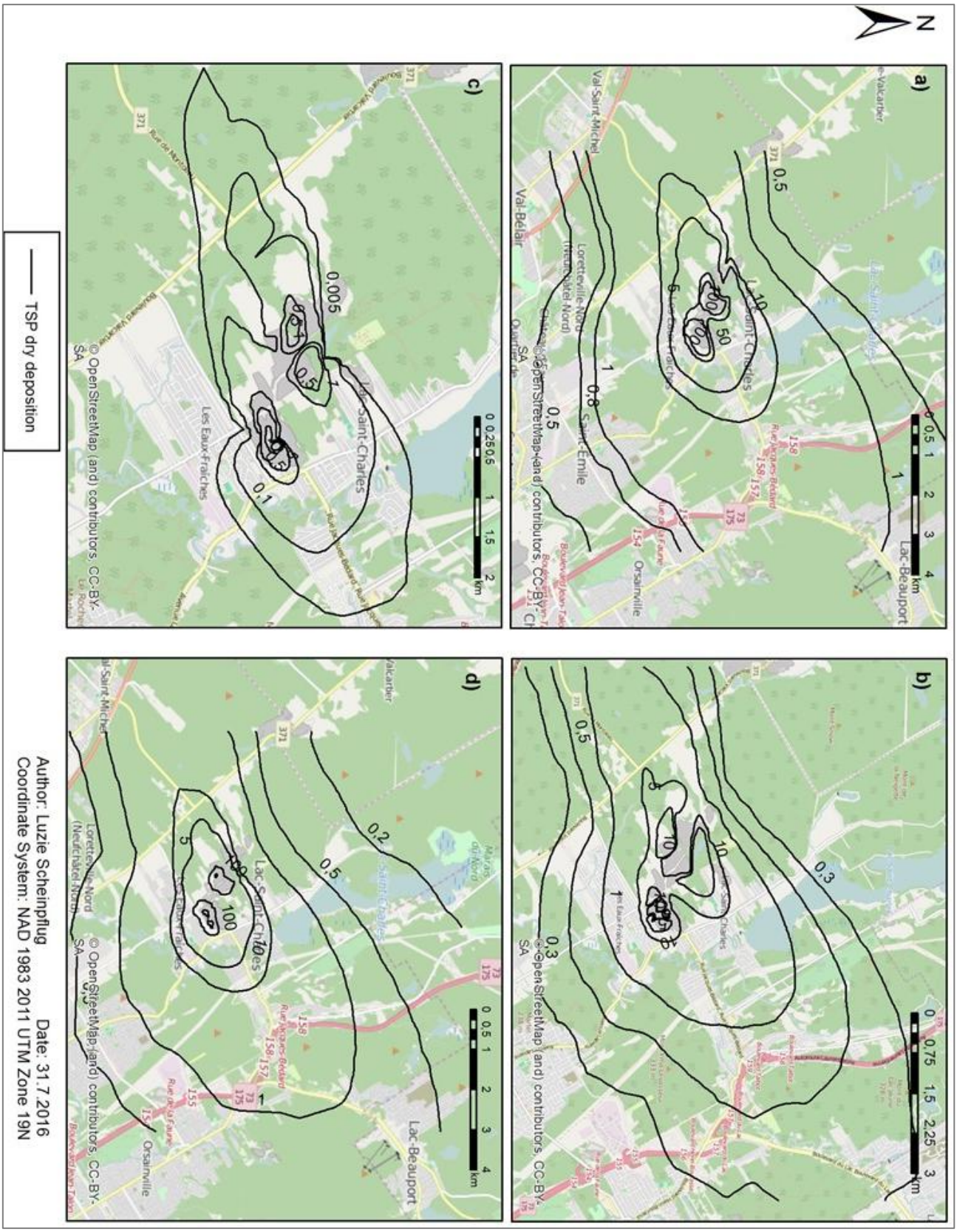

Figure 15: AERMOD modeling results of the TSP dry deposition (g/m^2). Figure 15a) represents the impact of all sources of the sand pit combined. Figure 15b) shows the significant contribution (just below half) of the two open pit sources to the total dry deposition. Figure 15c) shows the impact of wind erosion, which is considered negligible. The contributions of the line sources (truck passage on road segments) are shown in figure 15d), representing the most important source group of the total dry emissions reaching Lake Saint-Charles.

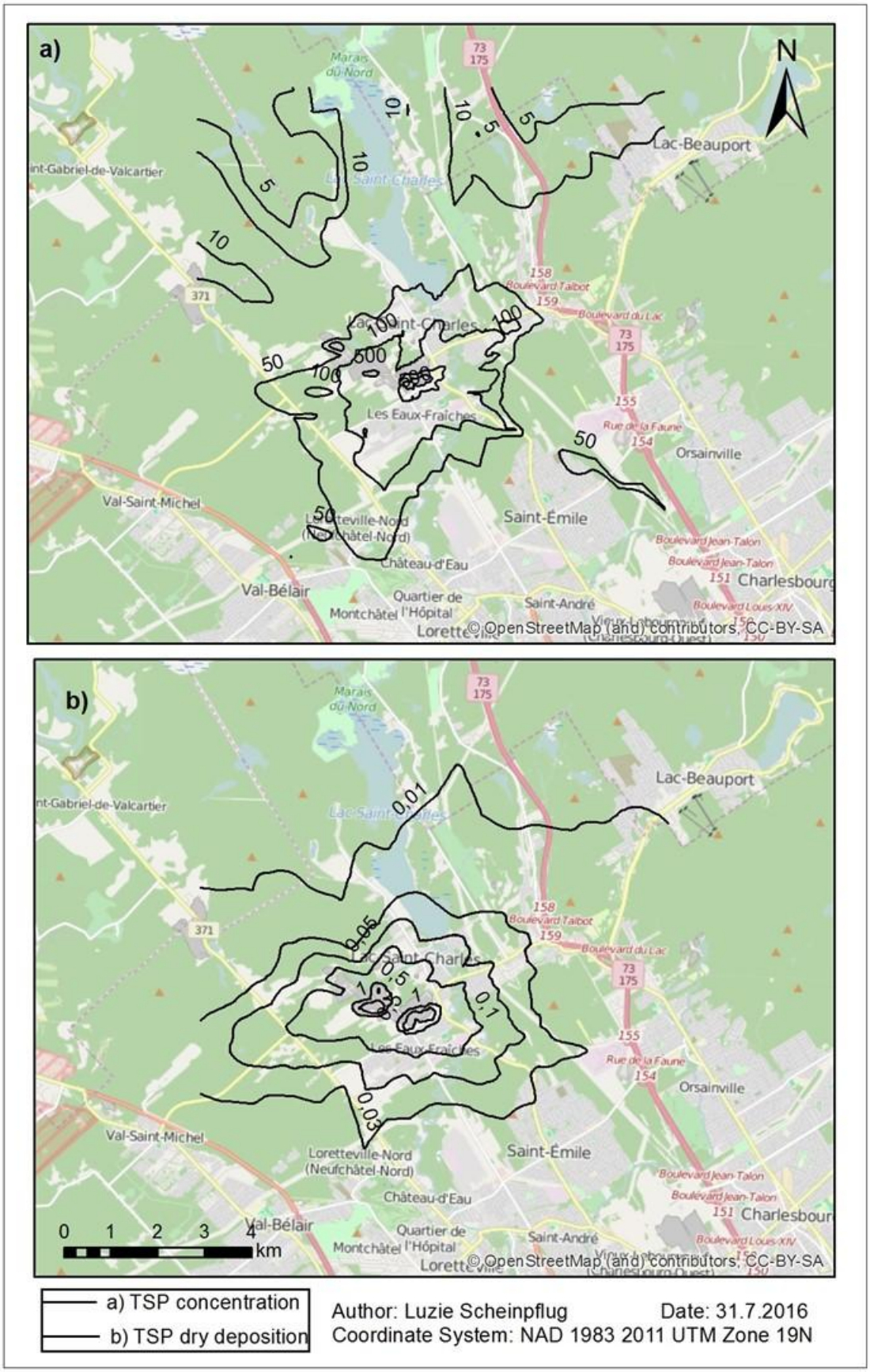

Figure 16: AERMOD modeling results of 24 hours maximum for TSP concentration in µg/m^3 (16a) and TSP dry deposition in g/m^2 (16b).

The province of Québec does not currently have an air quality standard concerning TSP dry deposition. As an alternative British Columbia's norms were taken into account. Table 22 compares norms with the highest modeled values for lake Saint-Charles. The yearly averaged modeled values are significantly below BC's standards (BC Ministry of Environment 2014). However, the 24 hours maximum (fig. 17) does show concentrations exceeding the norm in proximity to the sand pit. Although the concentration above the lake does not exceed the norm, it is still very elevated and not to be ignored. The modeled maximum 24 hours deposition is of no concern as the values are far below the BC norms.

Table 22: Highest modeled values for the lake for both concentration and dry deposition of TSP over a 24 hour period compared to air quality standards of Québec (QC) and British Columbia (BC), Canada. Source: BC Ministry of Environment 2014, MDDELCC 2016.

	Average Period	Air Quality Standard	Highest modeled value for the lake
TSP concentration	24 hour	120 µg/m^3 (QC)	59.76 µg/m^3
dustfall/dry deposition	month	1.7 mg/(dm^2-d) (BC)	0.5 mg/(dm^2-d)

In addition, the deposition onto lake Saint-Charles was calculated. It was estimated that 1.16 t of atmospheric dust prevalent from the sand pit fall into the entire water body per period (between mid-April and November).

3.2.3 Method discussion

A lack of information provoked a large scale assumption concerning the data basis of the modeling. Although trucks entering and leaving the sand pit were counted, no precise information of what happens inside the pit was available. Moisture and silt content, truck routes, active surface areas and heavy machinery were estimated. These circumstances could have led to under- or overestimation of particle quantities. A description of how certain parameters were deducted can be found in part 2.3.1 In addition, meteorological data was taken from the Québec's international airport Jean-Lesage which is 12 km south of the sandpit. A weather station in closer proximity would lead to more accurate results.

In addition the owners of the sand pit would need to release all information necessary to calculate precise emission rates. Since only one situation seen on a satellite is the basis for the modeling, temporal variations of the pit's activity cannot be accounted for. Although meteorological data over multiple years is used, the pit is assumed unchanged over the time frame. It has also been proven that AERMOD has a systematic underprediction of about 40% (Hanna 2001).

3.3 Comparison of field work and modeling results

The field work campaign and the modeling are not comparable after this explorative study. Field work data was collected over a much shorter and less representative time frame, whilst the model

represents a long term average. It is important to note that the measured values are collected over a 24 hours period, whilst the modeled values are only calculating values for 12 hours a day. The model would also need local meteorological data to be comparable to on-site measurements. In addition, the calculated emission rates were estimated and thus emissions might not represent actual pollution. APEL is confident to continue this project over the following years and perhaps rendering the two methodology branches comparable.

3.4 Potential limnological impact

This explorative study is part of a wider project to understand the ecological problems of lake Saint-Charles and its premature aging. Primary production in lake Saint-Charles has been rapidly increasing and atmospheric deposition of nutrients could be a significant contributor to the lake's organic carbon production. Thus it is important to discuss the limnological impact of the measured and modeled atmospheric deposition.

Atmospheric dust is a common source of nutrient influx, especially nitrogen (N) and phosphorus (P) (Ellis et al. 2015). In fact, on a global scale atmospheric dust contributes much more nitrogen to freshwater surfaces than rivers and is considered the dominant distribution process (Paerl 1998; Galloway et al. 2008). Apart from nitrogen and phosphorus, sulfate (SO_4) is often another product deposited through atmospheric dust and can lead to acidification (Ellis et al. 2015). Nitrogen depositions, especially NH_4 and NO_3, can render a lake acidic as the precursors of nitric acid (Vitousek et al. 1997). This is a problem for lakes with poor buffering capacities.

Spring and summer months are most prone to atmospheric loading and deposition of nitrogen, phosphorus and sulfates. A positive correlation between atmospheric concentration and deposition exists. A longer term, year-round study may prove elevated dust emissions even in the winter, which suggests important, but distant sources. Furthermore tributary loading is confined to specific spots in the lake and often penetrates into deeper water zones. Atmospheric loading is spread lake wide and impacts the photic zone (Ellis et al. 2015). According to Paerl (1997) external nitrogen may play an important part in noxious cyanobacteria blooms. Atmospheric deposition will especially affect the blue-green algae species *Anabaena flos-aquae*. This type represented the dominant species of cyanobacteria in Lake Saint-Charles in 2010, 2011 and 2012 (Rolland et al. 2013; APEL 2014). Many other cyanobacteria and aquatic plants will bloom with increased nutrient input (APEL 2014). Elser et al. (2009) argues that the increasing influx of inorganic nitrogen into freshwater lakes causes a shift from a natural nitrogen limitation to a phosphorus limitation by altering the natural N:P ratio. This results in reduced biodiversity and a decreased production of higher trophic levels (Elser et al. 2009). Specific contaminations and consequences of atmospheric loading into Lake Saint-Charles still needs to be researched.

4. Conclusion and Outlook

After an explorative modeling, atmospheric concentrations of TSP were found over lake Saint-Charles prevalent from the sand pit. Although they do not exceed air quality standards, their influence on the water quality and trophic state of the lake may still be significant, as air quality standards do not take impacts on ecosystems into account. The deposition of atmospheric dust prevalent from the sand pit onto the entire water body of Lake Saint-Charles was estimated at 1.16 t per period (between mid-April and November).

An increase of atmospheric particulate matter was directly measured north-east of the sand pit during the field work campaign, but could not be confirmed at the lake's border, where the concentration did not exceed the control. A long-term study needs to be undertaken to establish average quantities. All contaminants and their consequences need to be strictly monitored, even more so in lake Saint-Charles due to its use as a drinking water reservoir. Potential effects of atmospheric deposition such as cyanobacteria blooms and a proliferation of aquatic plants augment the price of water treatment significantly. Including all the ameliorations already stated, a thorough chemical analysis of the air samples would contribute a great deal to the understanding of what impacts the dust has on the lake. Suggestions for dust emission reductions from the sand pit include paving or watering roads on a daily basis, watering all other activities, reducing truck speeds and using chemical binding agents on the roads. Further information on mitigation strategies can be found in Gillies et al. (1999) and Norman & Johansson (2006).

The outlook of this project is to establish an improved method based on this explorative one to improve and refine results. A local meteorology tower is of utmost importance. Furthermore chemical compounds found on the filters need to be specifically searched for in the lake to establish a fundamental connection to atmospheric deposition. Based on the experience of this study, atmospheric deposition could be included in the long-term yearly monitoring of Lake Saint-Charles for all the surrounding sand and gravel pits. Nitrogen and sulfur compounds could not be analyzed in this study but need to be considered in the following years. Not much scientific research exists on the subject, so further studies would be necessary to contribute to cutting edge research. Table 23 summarizes method improvements for both field work and modeling, which need to be considered for follow-up studies.

Table 23: Method improvements to be considered for follow-up studies.

Field work campaign	Modeling
• Standardized local weather station • Include all sand pit surrounding the lake • Long-term sampling • Sampling frequency of three days all year-round • Preferably glass fiber or Teflon filters, to avoid under estimation • Elevate base-level station, VAL, to measure base level on a similar height as both other stations	• Standardized local weather station • Include all sand pits surrounding the lake • Complete knowledge on sand pit operations, including truck count and route, heavy machinery, excavated quantities, working hours • No model change, although AERMOD underestimates largely, it is the regulatory model in Québec

5. Acknowledgements

Firstly I would like to especially thank Sonja Behmel, Richard Leduc and Ralf Ludwig for their expertise, insight and mentoring during this project. I am thankful to my colleague Jimmy Duchesneau for assisting me in the field work campaign and APEL for organizing this study. Special thanks also go to Mr. Denis Blouin who graciously offered his backyard to create the field work station VAL. This project would have been impossible without the funding of the municipality of Québec City and the scholarships of AirMet Science Inc. and the Ludwig-Maximilians-University Munich. Thank you also to the Ministry of Sustainable Development, Environment and Climate Change for the loan of three high volume air filters. I am also grateful to Jesse Thé, Lakes Environmental Inc. who contributed the AERMOD trial license through AirMet Science Inc. I thank APEL for providing all other materials, transport and a work place.

IV. References

APEL (2009): *Étude limnologique du haut-bassin de la rivière Saint-Charles, rapport*. Association pour la protection de l'environnement du lac Saint-Charles et des Marais du Nord. Québec.

APEL (2014): *Mémoire: État du lac Saint-Charles*. Association pour la protection de l'environnement du lac Saint-Charles et des Marais du Nord. Québec.

APEL (2014): *Diagnose du lac Saint-Charles 2012.* Association pour la protection de l'environnement du lac Saint-Charles et des Marais du Nord. Québec.

AVANTI Mining Inc. (publisher) (2011): *Kitsault Mine Project Environmental Assessment - Appendix 6.2 C Atmospheric Environment - Emission Sources and Air Quality Modelling*. Toronto.

Bouchard M (1989): *Subglacial landforms and deposits in central and northern Québec, Canada, with emphasis on Rogen moraines*. In: Sedimentary Geology, 62/2-4, 293-308.

Bourget S (2011): *Limnologie et charge en phosphore d'un résevoir d'eau potable sujet à des fleurs d'eau de cyanobactéries: Le Lac Saint-Charles, Québec*. Master's thesis, University of Laval. Retrieved from theses.ulaval.ca/2011/28078/28078.pdf (25.4.2016).

British Columbia Ministry of Environment (2014): *Provincial Air Quality Objective Information Sheet*. British Columbia.

Carmichael W (2001): *Health effects of Toxin-Producing Cyanobacteria: "The CyanoHABs".* In: Human and Ecological Risk Assessment, 7/5, 1393-1407.

Csavina J, Field J, Taylor M, Gao S, Landázuri A, Betterton E and Sáez A (2012): A *Review on the Importance of Metals and Metalloids in Atmospheric Dust and Aerosol from Mining Operations*. In: Science of the Total Environment, 433, 58-73.

Cimorelli A, Perry S, Venkatram A, Weil J, Paine R, Wilson R, Lee R, Peters W and Brode R (2005): *AERMOD: A Dispersion Model for Industrial Source Applications. Part 1: General Model Formulation and Boundary Layer Characterization.* In: Journal of Applied Meteorology, 44/5, 694-708.

Chorus I, Falconer I, Salas H & Bartram J (2000): *Health risks caused by freshwater cyanobacteria in recreational waters.* In: Journal of Toxicology and Environmental Health, Part B: Critical Reviews, 3/4, 323-347.

Cox P, Banack S, Murch S, Rasmussen U, Tien G, Bidigare R, Metcalf J, Morrison L, Codd G & Bergman B (2005): *Diverse taxa of cyanobacteria produce beta-N-methylamino-l-alanine, a neurotoxic amino acid.* In: Proceedings of the National Academy of Sciences of the United States of America, 102/14, 5074-5078.

Dams R and Heindryckx R (1973): *A high-volume air sampling system for use with cellulose filters*. In: Atmospheric Environment, 7/3, 319-322.

Ecological Stratification Working Group (ESWG) (publisher) (1995): *A National Ecological Framework for Canada*. Agriculture and Agri-Food Canada, Research Branch, Centre for Land and Biological

Resources Research and Environment Canada, State of the Environment Directorate, Ecozone Analysis Branch, Ottawa/Hull. Report and national map at 1:7500 000 scale.

Environnement Canada (2015): Données des stations pour le calcul des normales climatiques au Canada de 1981 à 2010. URL: http://www.climat.meteo.gc.ca/climate_normals/results_1981_2010_f.html?stnID=5251&radius=25&proxSearchType=city&coordsCity=46|49|71|13|Qu%C3%A9bec&degreesNorth=&minutesNorth=&secondsNorth=&degreesWest=&minutesWest=&secondsWest=&proxSubmit=go&dCode=0 (Accessed 25/4/2016).

Ellis B, Craft J and Stanford J (2015): *Long-term atmospheric deposition of nitrogen, phophorus and sulfate in a large oligotrophic lake*. In: PeerJ, 3/4, e841.

Elser J, Andersen T, Baron J, Bergstrom A, Jansson M, Kyle M, Nydick K, Steger L and Hessen D (2009): *Shifts in lake N:P stoichiometry and nutrient limitation driven by atmospheric nitrogen deposition*. In: Science, 326/5954, 835–837.

Ernst B, Dietz L, Hoeger S and Dietrich D (2005): *Recovery of MC-LR in fish liver tissue.* In: Environmental Toxicology, 20/4, 449-458.

Field J, Belnap J, Breshears D, Nefff J, Okin G, Whicker J, Painter T, Ravi S, Reheis M and Reynolds R (2010): *The ecology of dust.* In: Front Ecological Environment, 8/8, 423-430.

DWA Deutsche Vereinigung fuer Wasserwirtschaft, Abwasser und Abfall e.V. (publisher), Fleckenstein J, Luo J, Miegel K, Nuetzmann G, Schoeniger M, Theis H, Wald J and Wittenberg H (2013): *Wechselwirkungen zwischen Grund- und Oberflaechenwasser*. In: DWA-Themen, T2.

Galloway J, Townsend A, Erisman J, Bekunda M, Zucong C, Freney J, Martinelli L, Seitzinger S, Sutton M (2008): *Transformation of the nitrogen cycle: recent trends, questions, and potential solutions.* In: Science, 320/5878, 889–892.

Galmarini S (2007): *Ensemble Dispersion Modelling: "All for one, One for All!"*. In: Borrego C and Norman A (publisher): Air Pollution Modeling and Its Application XVII. Springer, 371-378.

Gilette D, Adams J, Endo A, Smith D and Khil R (1980): *Threshold velocities for input of soil particles into the air by dessert soils.* In: Journal of Geophysical Research: Oceans, 85/C9, 5621-5630.

Glibert P, Maranger R, Sobota D and Bouwman L (2014): *The Haber Bosch - harmful algal bloom (HB-HAB) Link*. In: Environmental Research Letters, 9/10, 105001.

Goudie A and Middleton N (2006): *Desert dust in the global system*. Springer.

Grantz D, Garner J and Johnson D (2003): *Ecological effects of particulate matter*. In: Environment International, 29/2-3, 213-239.

Green M, Chen A, DuBois D and Molenar J (2012): *Fine particulate matter and visibility in the Lake Tahoe Basin: Chemical Charaterization, trends and source apportionment*. In: Journal of the Air & Waste Management Association. 62/8. 953-965.

Griffin D, Kellogg C, Shinn E (2001): *Dust in the wind: Long range transport of dust in the atmosphere and its implications for global public and ecosystem Health*. In: Global Change Human Health, 2/1, 20–33.

Hale C & Astolfi D (2015): *Evaluating Education and Training Services: A Primer*. St-Leo.

Hanna S, Egan B, Purdum J and Wagler J (2001): *Evaluation of the ADMS, AERMOD and ISC3 Dispersion Models with OPTEX, Duke Forest, Kincaid, Indianapolis and Lovett Field Data Set.* In: International Journal of Environment and Pollution, 16/, 1-6

Holmes N and Morawska L (2006): *A Review of Dispersion Modelling and its application to the dispersion of particles: An overview of different dispersion models available.* In: Atmospheric Environment, 40/30, 5902-5928.

Jones A (2004): *Atmospheric dispersion modeling at the Met Office.* In: Weather, 59/11, 311-316.

Juettner F and Watson S (2007): *Biochemical and ecological control of Geosmin and 2-Methylisoborneol in source waters.* In: Applied and Environmental Microbiology, 73/14, 4395-4406.

Lancaster N (2009): *Aeolian features and processes*. In: Young, R.S and Norby, L. (publisher): Geological Monitoring. Boulder. 1-26.

Magnuson J, Webster K, Assel R, Bowser C, Dillon P, Eaton J, Evans H, Fee E, Hall R, Mortsch L, Schindler D et Quinn F (1997). *Potential Effects of Climate Changes on Aquatic systems: Laurentian Great Lakes and Precambrian shield region*. In: Hydrological Processes, 11/8, 825-871.

Paerl H (1997): *Coastal eutrophication and harmful algal blooms: importance of atmospheric deposition and groundwater as new nitrogen and other nutrient sources.* In: Limnology and Oceanography, 42/5-2, 1154–1165.

Park R, Jacob D, Field B, Yantosca R and Chin M (2004): *Natural and transboundary pollution influences on sulfate-nitrate-ammonium aerosols in the United States: Implications for policy*. Journal of Geophysical Research, 109/D15204.

Peckenham J, Thornton T and Whalen B (2008): *Sand and gravel mining: effects on ground water resources in Hancock county, Maine, USA.* In: Environmental Geology, 56/6, 1103.

Pope C and Dockery D (2006): *Health effects of fine particulate air pollution: lines that connect*. Journal the Air & Waste Management Association, 56/6, 709–742.

Québec (publisher) (2016): *Vehicle Load and Size Limits Regulation*. Québec. (URL: http://legisquebec.gouv.qc.ca/en/pdf/cr/C-24.2,%20R.%2031.pdf (16.6.2016))

Reheis M, Budahn J, Lamothe P and Reynolds R (2009): *Compositions of modern dust and surface sediments in the Desert Southwest, United States*. In: Journal of Geophysical Research Earth Surface, 114/F01028.

Rolland D (2013): *La prolifération de cyanobactéries en réservoir tempéré nordique 9le Lac Saint-Charles, Québec. Canada): variabilité et facteurs de contrôle.* Doctoral Dissertation, University of Laval. Retrieved from theses.ulaval.ca/2013/30002/30002.pdf (5.5.2016).

Schlesinger W (1997): *Biogeochemistry - Analysis of Global Change*. San Diego.

Schultz J (2005): *The Ecozones of the World - The Ecological Divisions of the Geosphere*. Berlin.

Schwoerbel J and Brendelberger H (2013): *Einführung in de Limnologie*. Heidelberg.

SENES Consultants Limited (publisher) (2013): *Dust Impact Assessment of the McCormick Pit*. Richmond Hill.

Shao Y, Raupach M and Findlater P (1993): *Effect of saltation bombardment on the entrainment of dust by wind.* In: Journal of Geophysical Research Atmospheres, 97/D7, 12719-12726.

Shao Y (2008): *Physics and Modeling of Wind Erosion*. Springer.

Steffenson D (2008): *Economic cost of cyanobacterial blooms*. In: Hudnell and Kenneth (publisher): Cyanobacterial harmful blooms: State of the science and research needs. Springer. 855-865.

Stuut J, Smalley I and O'Hara-Dhand K (2009): *Aeolian dust in Europe: African sources and European deposits*. In: Quarternary International 198/1-2, 234-245.

Tremblay R, Légaré S, Pienitz R, Vincent W and Hall R (2001): *Étude paléolimnologique de l'histoire trophique du lac Saint-Charles, réservoir d'eau potable de la communauté urbaine de Québec*. In: Revue des sciences de l'eau, 14/4, 489-510.

Umwelt Bundesamt (UBA) (publisher) (2013): *Ausbreitungsmodelle fuer anlagenbezogee Immissionsprognosen.* URL: https://www.umweltbundesamt.de/themen/luft/regelungen-strategien/ausbreitungsmodelle-fuer-anlagenbezogene/uebersicht-kontakt (Accessed 1.8.2016).

United States Environmental Protection Agency (EPA) (publisher) (1995): *Compilation of Air Pollutant Emission Factors, Volume 1: Stationary point and area sources*. USA.

United States Environmental Protection Agency (EPA) (publisher) (2004): *AERMOD: Description of Model Formulation*. USA.

United States Environmental Protection Agency (EPA) (publisher) (2016): *Preferred/Recommended Models*. URL: https://www3.epa.gov/scram001/dispersion_prefrec.htm (Accessed 25/7/2016).

Van Pelt R and Zobeck T (2007): *Chemical constituents of fugitive dust.* In: Environmental Monitoring Assessment, 130/1-3, 3-16.

Venkatram A, Brode R, Cimorelli A, Lee R, Paine R, Perry S, Peters W, Weil J and Wilson R (2001): *A complex terrain dispersion model for regulatory applications.* In: Atmospheric Environment, 35/24, 4211-4221.

Vitousek P, Aber J, Howarth R, Likens G, Matson P, Schindler D, Schlesinger W and Tilman D (1997): *Human alteration of the global nitrogen cycle: sources and consequences*. In: Ecological Applications, 7/3, 737–750.

WSP Canada Inc. (publisher) (2014): *Modélisation de la dispersion atmosphérique Canadian Malartic GP - Project d'extension de la mine aurifère Canadian Malartic.* Trois-Rivières.

Yannopoulos S, Basbas S and Giannopoulou I (2013): *Water bodies pollution due to highways stormwater runoff: measures and legislative framework*. In: Global NEST Journal, 15/1, 85-92.

Zobeck T and Fryrear D (1986): *Chemical and physical characteristics of windblown sediment II. chemical characteristics and total soil and nutrient discharge*. In: Transactions of the ASAE, 29/4, 1037–1041.

V. APPENDIX A

Table 24 Complete field work results from the 15th of May to the 1st of August, including all wind directions

Date	Concentration (µm/m^3)			Dominant wind direction	Precipitation (mm)
	VAL	PEB	APEL		
15-05-2016	3.5	4.6	6.1	NE	18.0
18-05-2016	7.7	18.8	8.9	SSE	0.0
21-05-2016	22.6	38.6	31.8	SSE	0.0
24-05-2016	41.2	56.4	50	SSE	0.0
27-05-2016	23.2	32.8	27.9	S	6.9
30-05-2016	23	32.2	29.7	S	19.0
02-06-2016	21.3	n.a.	14.9	NW	16.0
05-06-2016	12.4	16.4	17.7	NW	28.4
08-06-2016	10.8	14.5	17.7	S	0.3
11-06-2016	10.6	19.3	11	S	0.0
14-06-2016	16.7	22.7	21.1	SSE	0.3
17-06-2016	33.7	40	10.8	NW	0.0
20-06-2016	35.9	123	26.8	NE	0.0
23-06-2016	13	24.8	124.7	S	0.0
26-06-2016	22.2	42.6	43.3	N	0.3
29-06-2016	13	12.7	32.5	NW	0.8
02-07-2016	9.5	12.9	11	NE	0.5
05-07-2016	25.6	51.8	52.6	NW	1.3
08-07-2016	14	29	22.9	W	0.0
11-07-2016	19.4	19.6	29.6	NE	0.0
14-07-2016	14.2	44.6	27.9	NE	10.2
17-07-2016	14.9	23.1	45.7	S	3.0
20-07-2016	13.3	28.5	20.3	NE	0.0
23-07-2016	13.6	15.6	11.3	S	0.0

26-07-2016	12.6	17.1	15.5	S	0.3
29-07-2016	11.9	17.4	7	S	0.0
01-08-2016	15.1	40.8	12	S	0.0

VI. APPENDIX B

As mentioned in this study, the chemical analysis (NO_3 and SO_4 concentrations) of collected TSP was done by EXOVA Inc. Canada. However, the results were not completed in time to be included in the study. The raw results (tab 25) and a quick statistical overview are thus presented here. Wind directions and precipitation data for the individual sampling days can be taken from table 24 in APPENDIX A. All results regardless of their wind direction were analysed with Sigma Plot.

Table 25 Results of SO_4 and NO_3 concentrations of the TSP samples.

Date	NO_3 Concentration (µm/m^3)			SO_4 Concentration (µm/m^3)		
	VAL	PEB	APEL	VAL	PEB	APEL
15-05-2016	0.05	0.05	0.10	3.1	3.3	3.8
18-05-2016	0.04	0.06	0.06	3.0	3.1	3.0
21-05-2016	0.14	0.17	0.17	7.1	5.7	5.6
24-05-2016	0.15	0.18	0.18	5.0	4.9	5.1
27-05-2016	0.19	0.27	0.25	4.2	4.6	4.3
30-05-2016	0.14	0.21	0.21	4.0	4.6	4.4
02-06-2016	0.12	0.07	0.10	3.1	3.0	3.1
05-06-2016	0.07	0.02	0.07	3.0	2.4	3.0
08-06-2016	0.02	0.14	0.02	2.5	3.3	2.5
11-06-2016	0.08	0.04	0.14	3.3	2.5	3.4
14-06-2016	0.02	0.12	0.04	2.6	2.4	2.6
17-06-2016	0.10	0.41	0.11	3.2	7.3	2.3
20-06-2016	0.24	0.04	0.39	4.6	1.9	7.4
23-06-2016	0.04	0.25	0.05	1.9	3.2	2.1
26-06-2016	0.17	0.08	0.25	3.2	2.6	3.6
29-06-2016	0.08	n.a	0.08	2.3	n.a	2.5

02-07-2016	0.06	0.08	0.08	2.5	2.5	2.6
05-07-2016	0.18	0.24	0.23	4.9	4.9	5.1
08-07-2016	0.06	0.06	0.06	1.8	1.9	1.8
11-07-2016	0.09	0.12	0.12	3.5	3.4	3.4
14-07-2016	0.19	0.28	0.26	4.9	5.0	5.2
17-07-2016	0.13	0.22	0.21	4.5	4.9	5.2
20-07-2016	0.05	0.08	0.07	3.5	4.0	3.7
23-07-2016	0.03	0.05	0.05	2.1	2.0	2.1
26-07-2016	0.07	0.11	0.11	2.8	2.6	2.6
29-07-2016	0.02	0.03	0.03	1.8	1.8	1.7
01-08-2016	0.04	0.06	0.05	2.2	2.3	2.3

As seen in figure 17, even with this small sampling size it becomes very clear that there is no significant difference in SO4 concentration between the field work stations.

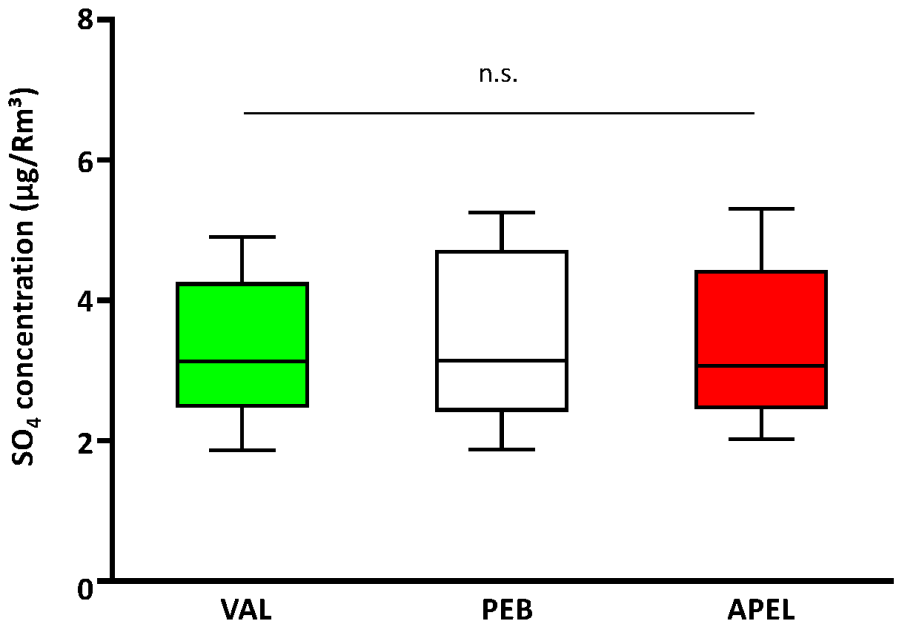

Figure 17 Statistical results of SO_4 concentrations showing no significant differences between the field work stations.

Concerning the NO_3 concentrations, no significant difference could be found. However, the test results are less clear and PEB and VAL may develop a significant difference with increased sample volume (fig 18).

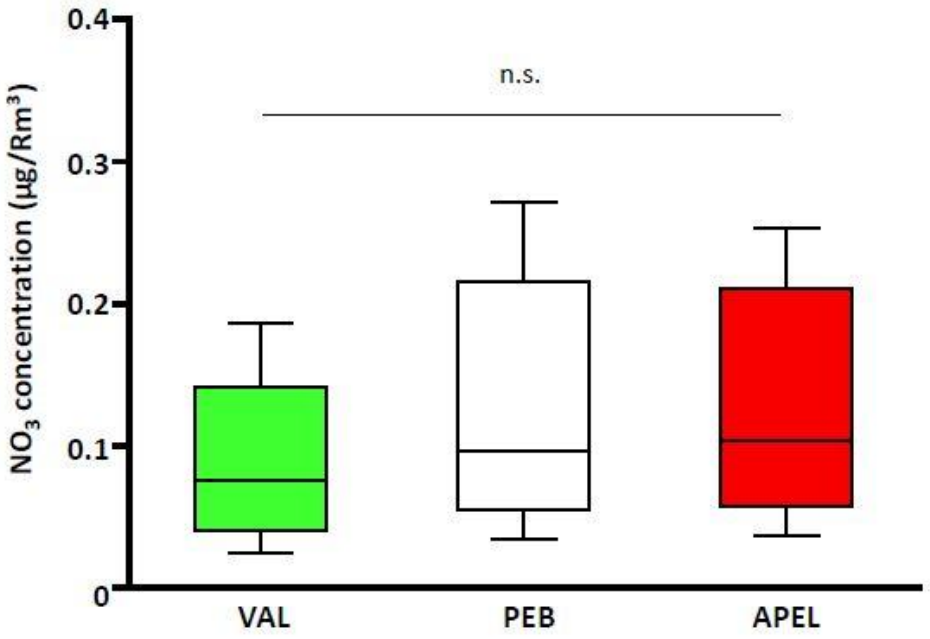

Figure 18 Statistical results of SO_4 concentrations showing no significant differences between the field work stations.